

1 In the submitted manuscript, we have substantially revised many sections based on the suggestions  
2 of the two reviewers. These revisions, along with responses to the reviewers' comments, are listed on  
3 a point-by-point basis in the "Final response to referees" document uploaded on 29<sup>th</sup> April.  
4 Additionally, we have revised the final manuscript such that it is more clearly guided by specific  
5 objectives and hypotheses. A fully marked version of the manuscript, showing all changes, is included  
6 below. In addition, we have submitted a "clean" version, through the online submission portal, for your  
7 consideration.

8

9 Sincerely,

10 James Bradley

11 **Microbial dynamics in a High-Arctic glacier forefield: a combined field, laboratory, and**  
12 **modelling approach.**

13 James A. Bradley <sup>1,2</sup>, Sandra Arndt <sup>2</sup>, Marie Šabacká <sup>1</sup>, Liane G. Benning <sup>3,4</sup>, Gary L. Barker <sup>5</sup>, Joshua  
14 J. Blacker <sup>3</sup>, Marian L. Yallop <sup>5</sup>, Katherine E. Wright <sup>1</sup>, Christopher M. Bellas <sup>1</sup>, Jonathan Telling <sup>1</sup>,  
15 Martyn Tranter <sup>1</sup>, Alexandre M. Anesio <sup>1</sup>

16  
17 <sup>1</sup> Bristol Glaciology Centre, School of Geographical Sciences, University of Bristol, BS8 1SS, UK

18 <sup>2</sup> BRIDGE, School of Geographical Sciences, University of Bristol, BS8 1SS, UK

19 <sup>3</sup> School of Earth and Environment, University of Leeds, LS2 9JT, UK

20 <sup>4</sup> GFZ, German Research Centre for Geosciences, 14473 Potsdam, Germany

21 <sup>5</sup> School of Biological Sciences, University of Bristol, BS8 1SS, UK

22

23 Corresponding author: James A. Bradley, email: j.bradley@bristol.ac.uk

24

25 **Abstract:** Modelling the development of soils in glacier forefields is necessary in order to assess how  
26 microbial and geochemical processes interact and shape soil development in response to glacier  
27 retreat. Furthermore, such models can help us predict microbial growth and the fate of Arctic soils in  
28 an increasingly ice-free future. Here, for the first time, we combined field sampling with laboratory  
29 analyses and numerical modelling to investigate microbial community dynamics in oligotrophic  
30 proglacial soils in Svalbard. We measured low bacterial growth rates and growth efficiencies (relative  
31 to estimates from Alpine glacier forefields), and high sensitivity to soil temperature (relative to  
32 temperate soils). We used these laboratory measurements to inform parameter values in a new  
33 numerical model and significantly refined predictions of microbial and biogeochemical dynamics of  
34 soil development over a period of roughly 120 years. The model predicted the observed accumulation  
35 of autotrophic and heterotrophic biomass. Genomic data indicated that initial microbial communities  
36 were dominated by bacteria derived from the subglacial environment, whereas older soils hosted a  
37 mixed community of autotrophic and heterotrophic bacteria. This finding was validated by the  
38 numerical model, which showed that active microbial communities play key roles in fixing and  
39 recycling carbon and nutrients. We also demonstrated the role of allochthonous carbon and microbial  
40 necromass in sustaining a pool of organic material, despite high heterotrophic activity in older soils.  
41 This combined field, laboratory and modelling approach demonstrates the value of integrated model-  
42 data studies to understand and quantify the functioning of the microbial community in an emerging  
43 High-Arctic soil ecosystem.

44

45 **Key words**

46 Glacier forefield

47 Microbial dynamics

48 Soil development

49 Numerical modelling

50 Integrated field-laboratory-modelling

51 SHIMMER

52  
53 **1. Introduction**

54 Polar regions are particularly sensitive to anthropogenic climate change (Lee, 2014) and have  
55 experienced accelerated warming in recent decades (Johannessen et al., 2004; Serreze et al., 2000;  
56 Moritz et al., 2002). The response of terrestrial Polar ecosystems to this warming is complex. Warmer  
57 conditions may increase soil respiration contributing to a positive feedback effect resulting from an  
58 increase in CO<sub>2</sub> efflux to the atmosphere. This will lead to further warming induced by the greenhouse  
59 effect (Billings, 1987; Oechel et al., 1993; Goulden et al., 1998). However, Arctic soils in particular  
60 may over several decades acclimatize to warming due to an increase in primary productivity,  
61 generating a net sink of CO<sub>2</sub> during the summer (Oechel et al., 2000). Accordingly, research to  
62 understand the response of terrestrial ecosystems in high latitudes to environmental change is of  
63 increasing importance. A visible consequence of Arctic warming is the large-scale retreat of glacier  
64 and ice cover (ACIA, 2005; Paul et al., 2011; Staines et al., 2014; Dyurgerov and Meier, 2000). From  
65 underneath the ice, a new terrestrial biosphere emerges, playing host to an ecosystem which may  
66 exert an important influence on biogeochemical cycles, and more specifically atmospheric CO<sub>2</sub>  
67 concentrations and associated climate feedbacks (Dessert et al., 2003; Anderson et al., 2000;  
68 Smittenberg et al., 2012; Berner et al., 1983). Furthermore, such a dramatic change will also  
69 invariably affect global methane budgets (Kirschke et al., 2013), the phosphorus cycle (Filippelli,  
70 2002; Follmi et al., 2009) and the productivity of downstream and coastal ecosystems (Anesio et al.,  
71 2009; Mindl et al., 2007; Fountain et al., 2008; Anderson et al., 2000).

72  
73 Numerous studies have attempted to characterize the physical and biological development of recently  
74 exposed soils using a chronosequence approach, whereby a transect perpendicular to the retreating  
75 ice snout represents a time sequence with older soils at increasing distance from the ice snout  
76 (Schulz et al., 2013). We have recently shown that microbial biomass and macronutrients (such as  
77 carbon, phosphorus and nitrogen) can accumulate in soils over timescales of decades to centuries  
78 (Bradley et al., 2014). In such pristine glacial forefield soils the activity of microbial communities is  
79 thought to be responsible for this initial accumulation of carbon and nutrients. Such an accumulation  
80 facilitates colonization by higher order plants, leading to the accumulation of substantial amounts of  
81 organic carbon (Insam and Haselwandter, 1989). However, organic carbon may also be derived from  
82 allochthonous sources such as material deposited on the soil surface (from wind, hydrology,  
83 precipitation and ornithogenic sources) and ancient organic pools derived from under the glacier  
84 (Schulz et al., 2013). Nevertheless, the relative significance of allochthonous and autochthonous  
85 sources of carbon to forefield soils, as well as their effect on ecosystem behavior are so far still poorly  
86 understood (Bradley et al., 2014). Moreover, cycling of bioavailable nitrogen (which is derived from  
87 active nitrogen-fixing organisms, allochthonous deposition, and degradation of organic substrates)  
88 and phosphorus (liberated from the weathering of minerals and decomposition of organic substrates)  
89 are similarly poorly quantified.

90

91 Several studies have observed shifts in the microbial community inhabiting pro-glacial soils of various  
92 ages (Zumsteg et al., 2012; Zumsteg et al., 2011). This was expressed in increasing rates of  
93 autotrophic and bacterial production with soil age (Schmidt et al., 2008; Zumsteg et al., 2013;  
94 Esperschütz et al., 2011; Frey et al., 2013) and the overall decline in quality of organic substrates in  
95 older soils (Goransson et al., 2011; Insam and Haselwandter, 1989). However, current evidence is  
96 limited to mostly descriptive approaches, which may be challenging to interpret due to inherent  
97 difficulties in disentangling interacting microbial and geochemical processes across various temporal  
98 and spatial scales. Furthermore, the inherent heterogeneity of glacial forefield soils makes the  
99 development of a single conceptual model that fits all challenging. Accordingly, pro-glacial  
100 biogeochemical processes that dominate such systems remain poorly quantified and highly under-  
101 explored. This current lack of understanding limits our ability to predict the future evolution of these  
102 emerging landscapes and the potential consequences on global climate. Numerical models present  
103 an opportunity to expand our knowledge of glacier forefield ecosystems by analytically testing the  
104 hypotheses that arise from observations, extrapolating, interpolating and budgeting processes, rates  
105 and other features to explore beyond the possibility of empirical observation (Bradley et al., 2016).  
106 With such a model we can then also explore the sensitivity and resilience of these ecosystems to  
107 environmental change.

108  
109 ~~To address this~~Here, we have combined field observations, with laboratory incubations and elemental  
110 measurements as well as genomic analyses and used these in a numerical model to investigate the  
111 development of soils in a glacial forefield. With this data we refined some model parameters in the  
112 recently developed **Soil biogeochemical Model for Microbial Ecosystem Response** (SHIMMER 1.0;  
113 Bradley et al. (2015)) model and applied this to the emerging forefield of the Midtre Lovénbreen  
114 glacier in Svalbard. The Midtre Lovénbreen forefield is an ideal site to test the field-laboratory-model  
115 approach due to the lack of vegetation during the first century of soil development, as this would  
116 obscure the microbial community dynamics and considerably alter the physical properties of the soil  
117 (Brown and Jumpponen, 2014; Ensign et al., 2006; King et al., 2008; Kastovska et al., 2005; Schutte  
118 et al., 2009; Duc et al., 2009). The model development was informed by decades of empirical  
119 research on glacier forefield soils, and has already been tested and validated using published  
120 datasets from the Damma Glacier in Switzerland and the Athabasca Glacier in Canada. A thorough  
121 sensitivity analysis highlighted the most important parameters to constrain in order to make further  
122 predictions more robust. All our model parameter values are specific to individual, local model  
123 conditions and inherently contain necessary model simplifications, abstractions and assumptions.  
124 Nevertheless, our earlier sensitivity analyses revealed the following highly sensitive key parameters  
125 as the most important to constrain through measurements: the maximum heterotrophic growth rate  
126 ( $I_{maxH}$ ), the bacterial growth efficiency (BGE, parameter  $Y_H$ ) and the temperature response ( $Q_{10}$ ).

127  
128 Therefore, in this current study, ~~we combined detailed field measurements with specifically designed~~  
129 ~~laboratory experiments and quantified values for these three parameters with a specific set of soils~~  
130 ~~from for the Midtre Lovénbreen forefield. The laboratory experiments and measurements were~~

Formatted: Font: 10 pt

Formatted: Font: 10 pt

131 ~~conducted with the objective to better constrain these sensitive parameters. We then ran model~~  
132 ~~simulations in order to explore the ranges of model output and refine model predictions. Next, we~~  
133 ~~examined model output to explore the microbial and biogeochemical dynamics of recently exposed~~  
134 ~~soils in the Midtre Lovénbreen catchment and evaluate two main hypotheses. First, we tested the~~  
135 ~~hypothesis that microbial biomass in recently exposed soils accumulates due to *in situ* bacterial~~  
136 ~~growth and activity. It is a commonly observed in glacier forefields that microbial biomass~~  
137 ~~accumulates with increasing soil age following exposure (Bernasconi et al., 2011; Schulz et al., 2013;~~  
138 ~~Bradley et al., 2014). This study provides a new quantitative and process-focused approach to~~  
139 ~~examine *in situ* growth in pioneer ecosystems, and assess the role of different functional groups in~~  
140 ~~biomass accumulation. Second, we tested the hypothesis that carbon fluxes in very recently exposed~~  
141 ~~soils are low, and are dominated by (abiotic) deposition of allochthonous substrate, whereas carbon~~  
142 ~~fluxes are high in older soils due to increased microbial (biotic) activity (such as microbial growth,~~  
143 ~~respiration and cell death). Increased soil carbon fluxes with soil age have been linked to microbial~~  
144 ~~activity from the forefield of the Damma Glacier, Switzerland (Smittenberg et al., 2012; Guelland et al.,~~  
145 ~~2013b). With this combined model, field and lab study, we were able to estimate carbon fluxes~~  
146 ~~between ecosystem components with daily resolution, and provide new insight into the interplay of~~  
147 ~~processes that contribute to net ecosystem production and soil organic carbon stocks in a High-Arctic~~  
148 ~~system.~~  
149 ~~we combined detailed field measurements with specifically designed laboratory experiments and~~  
150 ~~quantified values for these three parameters with a specific set of soils from for the Midtre Lovénbreen~~  
151 ~~forefield. With this data we have improved the confidence in our model predictions and assessed the~~  
152 ~~model performance. Finally, the model was used to explore microbial community structure and carbon~~  
153 ~~cycling dynamics in this High Arctic setting.~~

## 155 2. Methods

### 156 2.1. Study site and sampling

157 Midtre Lovénbreen is an Arctic polythermal valley glacier on the south side of Kongsfjorden, Western  
158 Svalbard (latitude 78°55'N, longitude 12°10'E) (Fig. 1). The Midtre Lovénbreen catchment is roughly 5  
159 km East of Ny-Ålesund, where several long-term monitoring programs have provided a wealth of  
160 contextual information. Midtre Lovénbreen has experienced negative mass balance throughout much  
161 of the 20<sup>th</sup> century. Since the end of the Little Ice Age (maximum in Svalbard in the 1900s) the de-  
162 glaciated surface area of the Midtre Lovénbreen catchment has increased considerably in response to  
163 warming mean annual temperatures. This continues to the present day. Between 1966 and 1990 ~  
164 2.3 km<sup>2</sup> of land was exposed (Fleming et al., 1997; Moreau et al., 2008). We used a chronosequence  
165 approach to determine ages for soils based on satellite imagery (Landsat TM 7) and previously  
166 determined soil ages by aerial photography and carbon-14 dating techniques in Hodkinson et al.  
167 (2003). Soil samples were collected along a transect perpendicular to the glacier snout, representing  
168 soil ages of 0, 3, 5, 29, 50, and 113 years (Fig. 1) during the field season (18 July to 29 August 2013).  
169 At each of the 6 sites along the chronosequence, 10 meter traverses roughly parallel to the glacier  
170 snout were established and at each site 3 soil plots were sampled (using ethanol sterilized sampling

Formatted: Font: 10 pt

Formatted: Font: 10 pt

Formatted: Font: 10 pt

Formatted: Font: 10 pt

Formatted: Font: 10 pt

Formatted: Font: 10 pt

Formatted: Font: 10 pt

Formatted: Font: 10 pt

Formatted: Font: 10 pt

Formatted: Font: 10 pt

Formatted: Font: 10 pt

Formatted: Font: 10 pt

Formatted: Font: 10 pt

171 equipment). After removing the > 2 cm rock pieces at each site, about 100 grams of soil was collected  
172 from the top 15 cm and immediately placed into sterile high-density polyethylene bags (Whirl-Pak  
173 (Lactun, Australia)) that were frozen and stored at -20°C, and transported to the laboratories in the  
174 Universities of Bristol and Leeds (UK).

175

## 176 **2.2. Laboratory analyses**

177 For bacterial abundance, samples were thawed and aliquots (100 mg) were immediately transferred  
178 into sterile 1.5 mL micro-centrifuge (Eppendorf) tubes, where they were diluted with 900 µL of Milli-Q  
179 water (0.2 µm filtered) and immediately fixed in 100 µL glutaraldehyde (0.2 µm filtered, 2.5% final  
180 concentration). Samples were then vortexed for 10 seconds and sonicated for 1 minute at 30°C to  
181 facilitate cell detachment from soil particles. Then, 10 µL of 100 µL fluorochrome DAPI (4', 6-diamidino-2  
182 phenylindole) was added to half of the samples, tubes were vortexed briefly (3 seconds) and  
183 incubated in the dark for 10 minutes, to be counted under UV light. The other half of each sample  
184 remained untreated, for counting under auto-fluorescent light for photosynthetic pigmentation.  
185 Samples were vortexed for 10 seconds and let stand for a further 30 seconds to ensure a well-mixed  
186 solution, prior to filtering 100 µL of the mixed liquid sample onto black Millipore Isopore membrane  
187 filters (0.2 µm pore size, 25 mm diameter), rinsed with a further 250 µL of Milli-Q water (0.2 µm  
188 filtered). Bacterial cells were then counted using an Olympus BX41 microscope at 1000 times  
189 magnification. The filtering apparatus was washed out with Milli-Q water between each filtration, and  
190 negative control samples, prepared using Milli-Q water, were included into each series. A negative  
191 control was a sample with no visible stained or auto-fluorescing cells. Thirty random grids (each 10<sup>4</sup>  
192 µm<sup>2</sup>) were counted per sample. Cell morphologies were measured and cell volume was estimated  
193 and converted to carbon content according to Bratbak and Dundas (1984) (see Supplementary  
194 Information). Separate aliquots of soil from each site were weighed after thawing and then dried at  
195 105°C to obtain an estimate of soil moisture content.

196

197 Environmental DNA was isolated from at least 3 replicates for each soil age using MoBio PowerSoil®  
198 DNA Isolation Kit and by following the instruction manual. The isolated 16S rDNA was amplified with  
199 bacterial primers 515f (5'-GTGYCAGCMGCCGCGTAA-3') and 926r (5'-  
200 CCGYCAATTYMTTTRAGTTT-3'), creating a single amplicon of ~400 bp. The reaction was carried  
201 out in 50 µL volumes containing 0.3 mg mL<sup>-1</sup> Bovine Serum Albumin, 250 µM dNTPs, 0.5 µM of each  
202 primer, 0.02 U Phusion High-Fidelity DNA Polymerase (Finnzymes OY, Espoo, Finland) and 5x  
203 Phusion HF Buffer containing 1.5 mM MgCl<sub>2</sub>. The following PCR conditions were used: initial  
204 denaturation at 95°C for 5 minutes, followed by 25 cycles consisting of denaturation (95°C for 40  
205 seconds), annealing (55°C for 2 minutes) and extension (72°C for 1 minute) and a final extension step  
206 at 72°C for 7 minutes. Samples were sequenced using the Ion Torrent platform (using Ion 318v2 chip)  
207 at Bristol Genomics facility at the University of Bristol. A non-barcoded library was prepared from the  
208 amplicon pool using Life technologies Short Amplicon Prep Ion Plus Fragment Library Kit. The  
209 template and sequencing kits used were: Ion PGM Template OT2 400 Kit and Ion PGM Sequencing  
210 400 kit. The sequencing yielded 4.38 million reads. The 16S sequences were further processed using

211 MOTHUR (v. 1.35) and QIIME pipelines (Schloss et al., 2009; Caporaso et al., 2010). Chimeric  
212 sequences were identified and removed using UCHIME (Edgar et al., 2011) and reads were clustered  
213 into operational taxonomical units (OTUs), based on at least 97% sequence similarity, and assigned  
214 taxonomical identification against Greengenes bacterial database (McDonald et al., 2012).

215

216 The carbon contents in the year 0 soils were analyzed with a Carlo-Erba elemental analyzer  
217 (NC2500) at the German Research Center for Geosciences, Potsdam, Germany. The ~~as-collected~~  
218 soils were oven dried at 40°C for 48 hours, sieved to <7 mm and crushed using a TEMA disk mill to  
219 achieve size fractions of < 20 µm. Total organic carbon (TOC) was analyzed after reacting the  
220 powders with a 10% HCl solution for 12 hours to remove inorganic carbonates.

221

### 222 2.3. Determination of maximum growth rates

223 ~~The microbial activity was determined in 113 year old soil samples after they were thawed (in the dark~~  
224 ~~at 5°C to mimic typical field temperature) for 168 hours. This age was chosen because these soil~~  
225 ~~samples were assumed to be the ones with the highest microbial biomass and activity and thus the~~  
226 ~~most appropriate for all laboratory measurements. In order to mitigate the effect of variability derived~~  
227 ~~from differences in soil properties between soil ages (that will later be predicted by the model),~~  
228 ~~laboratory experiments were conducted on a single soil age, with replicate incubations to assess the~~  
229 ~~possible variability in rates (and thus parameter values) that can be attributed to experimental~~  
230 ~~procedures and measurement techniques.~~

231 ~~The microbial activity was determined in 113-year old soil samples after they were thawed (in the dark~~  
232 ~~at 5°C to mimic typical field temperature) for 168 hours. This age was chosen because these soil~~  
233 ~~samples were assumed to be the ones with the highest microbial biomass and activity and thus the~~  
234 ~~most appropriate for all laboratory measurements.~~

235 Aliquots of the soils were divided into petri dishes (25 g of soil (wet weight) into each petri dish) for  
236 subsequent treatments. In order to alleviate nutrient limitations and measure maximum growth rates,  
237 four different nutrient conditions were simulated: (1) no addition of nutrients, (2) low (0.03 mg C g<sup>-1</sup>,  
238 0.008 mg N g<sup>-1</sup>, 0.02 mg P g<sup>-1</sup>), (3) medium (0.8 mg C g<sup>-1</sup>, 0.015 mg N g<sup>-1</sup>, 0.1 mg P g<sup>-1</sup>) and (4) high  
239 additions (2.4 mg C g<sup>-1</sup>, 0.024 mg N g<sup>-1</sup>, 0.3 mg P g<sup>-1</sup>). The ranges and concentrations were informed  
240 by similar experiments in recently exposed proglacial soils at the Damma Glacier, Switzerland  
241 (Goransson et al., 2011). Nutrients (C<sub>6</sub>H<sub>12</sub>O<sub>6</sub> for C, NH<sub>4</sub>NO<sub>3</sub> for N and KH<sub>2</sub>PO<sub>4</sub> for P) (Sigma, quality  
242 ≥99.0%) were dissolved in 2 mL Milli-Q water (0.2 µm filtered), and mixed into the soils using an  
243 ethanol-sterilized spatula. Samples were incubated at 25°C (~~for later comparison of growth rates with~~  
244 ~~previous estimates (Frey et al., 2010) in keeping with the design of SHIMMER and for comparison with~~  
245 ~~previous plausible range~~ (Bradley et al., 2015; Frey et al., 2010)) in the dark for a further 72 hours  
246 with the lids on. Throughout the whole incubation time, at 24 hour intervals, additional 2 mL aliquots of  
247 Milli-Q water (0.2 µm filtered) were added to maintain approximate soil moisture conditions in each  
248 sample.

249

250 In these samples bacterial production was estimated by the incorporation of  $^3\text{H}$ -leucine using the  
251 microcentrifuge method detailed in Kirchman (2001). After the initial 72 hour incubation period  
252 quadruplicate sample aliquots from the petri dish incubations and two trichloroacetic acid (TCA) killed  
253 control samples were incubated for 3 hours at 25°C for every nutrient treatment. Approximately 50 mg  
254 of soil was transferred to sterile micro-centrifuge tubes (2.0 mL, Fischer Scientific). Milli-Q (0.2  $\mu\text{m}$   
255 pre-filtered) water and  $^3\text{H}$ -leucine was added to a final concentration of 100 nM (optimum leucine  
256 concentration was pre-determined by a saturation experiment, Fig. S1, Supplementary Information).  
257 The incubation was terminated by the addition of TCA to each tube. Tubes were then centrifuged at  
258 15,000 g for 15 minutes, the supernatant was aspirated with a sterile pipette and removed, and 1 ml  
259 ice-cold 5% TCA was added to each tube. Tubes were then centrifuged again at 15,000g for 5  
260 minutes, before again aspirating and removing the supernatant. 1mL ice-cold 80% ethanol was added  
261 and tubes were centrifuged at 15,000 g for 5 minutes, before the supernatant was aspirated and  
262 removed again and tubes were left to air dry for 12 hours. Finally, 1 mL of scintillation cocktail was  
263 added, samples were vortexed, and then counted by liquid scintillation (Perkin Elmer Liquid  
264 Scintillation Analyzer, Tri-Carb 2810 TR). Radioisotope activity of TCA-killed control samples was  
265 always less than 1.1% of the measured activity in live samples. There was a positive correlation  
266 between the amount of sediment added to the tubes and background counts representing  
267 disintegrations per minute (DPM). Counts were individually normalized by the amount of sediments  
268 (corrected for dry weight) used in each sample to discount for background DPM. Leucine  
269 incorporation rates were converted into bacterial carbon production following the methodology of  
270 Simon and Azam (1989). Bacterial abundance was estimated from each treatment after the 72 hour  
271 incubation period by microscopy. Five samples from each petri dish were counted for each nutrient  
272 treatment with negative controls yielding no detectable cells. One-way ANOVA (with post-hoc Tukey  
273 HSD) statistical tests were used for evaluations of the variability from the multiple treatments.

274

#### 275 **2.4. Temperature response**

276 Microbial community respiration was determined by measuring  $\text{CO}_2$  gas exchange rates in airtight  
277 incubation vials. Soil samples from the 113 year old site were defrosted and divided (25 g wet weight)  
278 in petri dishes as above, and 2 mL of Milli-Q water (0.2  $\mu\text{m}$  filtered) was added (to maintain  
279 consistency of soil moisture with determination of bacterial production above). Samples were  
280 incubated at 5°C ( $T_1$ ) and 25°C ( $T_2$ ) in the dark for a further 72 hours. 2mL of 0.2  $\mu\text{m}$  pre-filtered Milli-  
281 Q water was added to the  $T_1$  sample (3 mL for  $T_2$ ) at 24, 48 and 72 hours to maintain approximate soil  
282 moisture content. Two separate killed control tests (one furnaceed at 450°C for 4 hours, and one  
283 autoclaved (3 cycles at 121°C)) were incubated at  $T_1$  and  $T_2$ . Quintuple live and killed samples  
284 (roughly 1 g) were transferred into cleaned 20 mL glass vials (rinsed in 2% Decon, submersed in 10%  
285 HCl for 24 hours, rinsed 3 times with Milli-Q water and furnaceed at 450°C for 4 hours). These were  
286 sealed (9°C, atmospheric pressure, ambient  $\text{CO}_2$  of 405 ppm) with pre-sterilized Bellco butyl stoppers  
287 (pre-sterilized by boiling for 4 hours in 1M sodium hydroxide) and crimped shut with aluminum caps.  
288 Sealed vials were then incubated at  $T_1$  and  $T_2$  for 24 hours in darkness. After 24 hours, the  
289 headspace gas was removed with a gas-tight syringe and immediately analyzed on an EGM4 gas



290 analyzer (PP Systems, calibrated using gas standards matching the expected range, precision 1.9%,  
291 2\*SE). Empty pre-sterilized vials were also incubated and analyzed. Following gas analysis, vials  
292 were opened and dried to a constant weight at 105°C to estimate moisture content and thus dry soil  
293 weight of these aliquots. Headspace CO<sub>2</sub> change (ppm) was converted to microbial respiration using  
294 the ideal gas law ( $n=PV/RT$ ), assuming negligible changes in soil pore water pH (and therefore CO<sub>2</sub>  
295 solubility) during the incubation. CO<sub>2</sub> headspace changes resulting from killed controls and blanks  
296 were < 70% of the changes resulting from the incubations at T<sub>1</sub>, and <7% of the changes observed at  
297 T<sub>2</sub>. One-way ANOVA (with post-hoc Tukey HSD) statistical tests were used for comparison of  
298 multiple treatments. No significant differences in CO<sub>2</sub> headspace change between killed controls at T<sub>1</sub>  
299 and T<sub>2</sub> were detected ( $P \geq 0.05$ ).

300

## 301 2.5. Microbial Model: SHIMMER

302 SHIMMER (Bradley et al., 2015) mechanistically describes and predicts transformations in carbon,  
303 nitrogen and phosphorus through aggregated components of the microbial community as a system of  
304 interlinked ordinary differential equations. [The model contains pools of microbial biomass, organic  
305 matter and both dissolved inorganic and organic nitrogen and phosphorus \(Table 1\).](#) ~~The model is 0-D  
306 and represents the soil as a homogeneous mix. Thus, light, temperature, nutrients, organic  
307 compounds and microbial biomass are assumed to be evenly distributed.~~ It categorizes microbes into  
308 autotrophs (A<sub>1-3</sub>) and heterotrophs (H<sub>1-3</sub>), and further subdivides these based on 3 specific functional  
309 traits. Microbes derived from underneath the glacier (referred to as “subglacial microbes”) are termed  
310 A<sub>1</sub> and H<sub>1</sub>. A<sub>1</sub> are chemolithoautotrophic, obtaining energy from the oxidation and reduction of  
311 inorganic compounds and carbon from the fixation of carbon dioxide. In contrast, H<sub>1</sub> rely on the  
312 breakdown of organic molecules for energy to support growth. A<sub>2</sub> and H<sub>2</sub> represent autotrophic and  
313 heterotrophic microbes commonly found in glacier forefield soils with no “special” characteristics, and  
314 will be referred to as “soil microbes”. A<sub>3</sub> and H<sub>3</sub> are autotrophs and heterotrophs that are able to fix  
315 atmospheric N<sub>2</sub> gas as a source of nitrogen in cases when dissolved inorganic nitrogen (DIN) stocks  
316 become limiting. Available organic substrate is assumed to be derived naturally from dead organic  
317 matter and allochthonous inputs. Labile compounds are immediately available fresh and highly  
318 reactive material, rapidly turned over by the microorganisms (S<sub>1</sub>, ON<sub>1</sub>, OP<sub>1</sub>). Refractory compounds  
319 are less bioavailable and represents the bulk of substrate present in the non-living organic component  
320 of soil (S<sub>2</sub>, ON<sub>2</sub>, OP<sub>2</sub>). [A conceptual diagram showing the components and transfers of SHIMMER is  
321 presented in the Supplementary Information \(Fig. S2\).](#)

322

323 Microbial biomass responds dynamically to changing substrate and nutrient availability (expressed as  
324 Monod-kinetics), as well as changing environmental conditions (such as temperature and light). A Q<sub>10</sub>  
325 temperature response function ( $T_i$ ) is affixed to all metabolic processes including growth rates and  
326 death rates (Bradley et al., 2015), thus effectively slowing down or speeding up all life processes as  
327 temperature changes (Soetaert and Herman, 2009; Yoshitake et al., 2010; Schipper et al., 2014).  
328 Light limitation is expressed as Monod kinetics.

329

330 The following external forcings drive and regulate the system's dynamics:  
331 • Photosynthetically-active radiation (PAR) (wavelength of approximately 400 to 700 nm) ( $W m^{-2}$ ).  
332  
333 • Snow depth (m).  
334 • Soil temperature ( $^{\circ}C$ ).  
335 • Allochthonous inputs ( $\mu g g^{-1} day^{-1}$ ).

336  
337 The model is 0-D and represents the soil as a homogeneous mix. Thus, light, temperature, nutrients,  
338 organic compounds and microbial biomass are assumed to be evenly distributed.  
339

340 Soil temperature (at 1 cm depth) for the entire of 2013 is provided by Alfred Wegener Institute for  
341 Polar and Marine Research (AWI) from the permafrost observatory near Ny-Ålesund, Svalbard.  
342 Similarly, PAR for 2013 are measured at the AWI surface radiation station near Ny-Ålesund,  
343 Svalbard. Averaged daily snow depth for 2009 to 2013 is provided by the Norwegian Meteorological  
344 Institute (eKlima). Allochthonous nutrient fluxes (inputs and leaching) are estimated based on an  
345 evaluation of nutrient budgets of the Midtre Lovénbreen catchment (Hodson et al., 2005) in which  
346 budgets for nutrient deposition rates and runoff concentrations are measured over two full summer-  
347 winter seasons and residual retention rates (excess of inputs) or depletion rates (excess of outputs)  
348 are inferred. The bioavailability of allochthonous material is assumed to be the same as initial material  
349 and microbial necromass.  
350

351 Initial conditions were informed by analysis of 0-years-of-exposure soil collected adjacent to the ice  
352 snout, and initial values for all state variables are presented in Table 1. Initial microbial biomass was  
353 estimated by microscopy as described above. Initial community structure was derived by 16S analysis  
354 of year-0 soils. An initial value for carbon substrate ( $S_1 + S_2$ ) was estimated based on the average  
355 TOC content of year-0 soil. Bioavailability of model TOC was assumed to be 30% labile ( $S_1$ ) and 70%  
356 refractory ( $S_2$ ) (for consistency with Bradley et al. (2015)). Organic nitrogen (ON) and organic  
357 phosphorus (OP) were assumed to be stoichiometrically linked by the measured C:N:P ratio from the  
358 Damma Glacier forefield (from which the model was initially developed and tested (Bradley et al.,  
359 2015)). An initial value for DIN was taken from a previous evaluation of Svalbard tundra nitrogen  
360 dynamics, whereby the lowest value is taken to represent the soil of least development, according to  
361 traditional understanding of glacier forefields (Alves et al., 2013; Bradley et al., 2014). An initial value  
362 for dissolved inorganic phosphorous (DIP) was established stoichiometrically from previous model  
363 development and testing.

364  
365 Model implementation and set-up is described in more detail in the Supplementary Information.  
366

## 367 2.6. Model parameters

368 Maximum heterotrophic growth rate  $I_{maxH}$  ( $day^{-1}$ ) was estimated by scaling the measured rate of  
369 bacterial production ( $\mu g C g^{-1} day^{-1}$ ) (converted to dry weight) with total heterotrophic biomass ( $\mu g C g$

Formatted: Subscript

Formatted: Subscript

370 <sup>1</sup>). Nutrient addition alleviates growth limitations as defined in SHIMMER (Bradley, 2015); thus  
371 bacterial communities can be assumed to be growing at  $I_{maxH}$  under experimental conditions.

372

373  $Y_H$  represents heterotrophic BGE, and was estimated according to the equation:

374

$$375 \quad Y_H = \frac{BP}{BP + BR} \quad (1)$$

376 Where  $BP$  is and  $BR$  are measured bacterial production and measured bacterial respiration ( $\mu\text{g C g}^{-1}$   
377  $\text{day}^{-1}$ ) respectively, at 25°C with no nutrients added.

378

379 The temperature response ( $Q_{10}$ ) value was estimated as:

380

$$382 \quad Q_{10} = \left(\frac{R_2}{R_1}\right)^{\left(\frac{10}{T_2 - T_1}\right)} \quad (2)$$

383 Where  $R_1$  and  $R_2$  represent the measured respiration rate ( $\mu\text{g C g}^{-1} \text{day}^{-1}$ ) at temperatures  $T_1$  and  $T_2$   
384 (5°C and 25°C).

385

386 Laboratory-defined parameters (i.e. growth rate, temperature sensitivity and BGE) were assumed to  
387 be the same for all microbial groups. A complete list of parameters and values is presented in Table  
388 S3 (Supplementary Information).

389

### 390 3. Results

#### 391 3.1. Laboratory results and model parameters

392 Bacterial production in untreated soil was estimated at  $0.76 \mu\text{g C g}^{-1} \text{day}^{-1}$  (SD=0.12), and across all  
393 nutrient treatments ranged from  $0.560$  to  $2.196 \mu\text{g C g}^{-1} \text{day}^{-1}$ . Nutrient addition led to increased  
394 measured production (low =  $0.69 \mu\text{g C g}^{-1} \text{day}^{-1}$  (SD=0.12), medium =  $1.09 \mu\text{g C g}^{-1} \text{day}^{-1}$  (SD=0.53),  
395 high =  $1.52 \mu\text{g C g}^{-1} \text{day}^{-1}$  (SD=0.63)), however variability between replicates was also high and  
396 production rates from each nutrient treatment were not significantly different from untreated soil ( $P_{\text{low}}=0.99$ ,  $P_{\text{medium}}=0.70$ ,  $P_{\text{high}}=0.10 > 0.05$ ). The increased bacterial production was cross-correlated  
397 with quadruplicate measurements of biomass from each treatment, and resulting growth rates for all  
398 treatments were within a narrow range ( $0.359$  to  $0.550 \text{day}^{-1}$ ) and there was no statistically significant  
399 difference in growth rates between each nutrient treatment (Fig. 2b) ( $P_{\text{low-medium}} \leq 0.05$ ,  $P_{\text{medium-high}}=0.49$ ,  $P_{\text{none-high}}=0.10$ ). The maximum measured growth rate for a single nutrient treatment, thus  
400 equating to the parameter  $I_{maxH}$ , was  $0.55 \text{day}^{-1}$ . The 95% confidence range for  $I_{maxH}$  is  $0.50$  to  $0.60$   
401  $\text{day}^{-1}$ . This value is, to our knowledge, is the first measured rate of bacterial growth from High-Arctic  
402 soils, and falls within the lower end of the plausible range established in Bradley et al. (2015) ( $0.24 -$   
403  $4.80 \text{day}^{-1}$ ) (Fig. 3a) for soil microbes from a range of laboratory and modelling studies (Fig. 5a) (Frey  
404 et al., 2010; Ingwersen et al., 2008; Knapp et al., 1983; Zelenev et al., 2000; Stapleton et al., 2005;  
405 Darrah, 1991; Blagodatsky et al., 1998; Vandewerf and Verstraete, 1987; Foereid and Yearsley,

Formatted: Subscript

Formatted: Subscript

Formatted: Subscript

Field Code Changed

409 [2004; Toal et al., 2000; Scott et al., 1995](#)). For respiration, significantly higher CO<sub>2</sub> headspace  
410 concentrations were detected in the live incubations at 25°C relative to killed controls (P < 0.05).  
411 Average respiration rate at 5°C was 1.61 C g<sup>-1</sup> day<sup>-1</sup> and there was a significant increase in soil  
412 respiration at 25°C (12.83 µg C g<sup>-1</sup> day<sup>-1</sup>) (Fig. 2c) (P < 0.05). The Q<sub>10</sub> value for Midtre Lovénbreen  
413 forefield soils was thus calculated as 2.90, and a 95% confidence range was established as 2.65 to  
414 3.16. [This was at the upper end of the plausible range previously identified in Bradley et al. \(2015\)](#)  
415 [\(Fig. 3b\)](#). Based on measured values of bacterial production and respiration, BGE (Y<sub>H</sub>) was 0.06, with  
416 a 95% confidence range of 0.05 to 0.07 [\(Fig. 3c\)](#). Final calculated values for model parameters are  
417 summarized in Table S3 (Supplementary Information).

418  
419 The results from microscopy determination of biomass are presented in Table 2. In the freshly  
420 exposed soil (year 0) heterotrophic biomass was low (0.059 µg C g<sup>-1</sup>), increased substantially to 0.244  
421 µg C g<sup>-1</sup> in 29 year old soils, and was an order or magnitude higher (2.00 µg C g<sup>-1</sup>) in 113 year old  
422 soils. Autotrophic biomass was considerably higher than heterotrophic biomass and increased by  
423 roughly an order of magnitude from year 0 (0.171 µg C g<sup>-1</sup>) to year 29 (1.07 µg C g<sup>-1</sup>) and  
424 approximately doubled by year 113 (2.58 µg C g<sup>-1</sup>). TOC in freshly exposed soil was approximately  
425 0.793 mg C g<sup>-1</sup>.

426  
427 16S data was categorized into microbial groups (A<sub>1-3</sub> and H<sub>1-3</sub>) as defined by the model formulation.  
428 Chemolithotrophs, such as known iron or sulfur oxidizers (genera [Acidothiobacillus](#), [Thiobacillus](#),  
429 [Gallionella](#), [Sulfurimonas](#)) were assigned into the A<sub>1</sub> group. Phototrophic microorganisms, such as  
430 cyanobacteria ([Phormidium](#), [Leptolyngbya](#)) and phototrophic bacteria ([Rhodospirillum rubrum](#), [Erythrobacter](#),  
431 [Halomicronema](#)) were allocated into group A<sub>2</sub>, while heterocyst forming cyanobacteria from the  
432 orders Nostocales and Stigonematales were assigned to group the A<sub>3</sub> (nitrogen-fixing autotrophs).  
433 Members of the family Comamonadaceae of the Betaproteobacteria are known subglacial dwelling  
434 microorganisms (Yde et al., 2010) and were thus included into the group H<sub>1</sub>. General soil  
435 heterotrophic microorganisms (mainly members of Alphaproteobacteria, Actinobacteria,  
436 Bacteroidetes and Acidobacteria) were assigned into group H<sub>2</sub> (general soil heterotrophs). Lastly,  
437 group H<sub>3</sub> consisted of heterotrophic nitrogen fixers, mainly [Azospirillum](#), [Bradyrhizobium](#), [Devosia](#),  
438 [Clostridium](#), [Frankia](#) and [Rhizobium](#). Pathogens, non-soil microorganisms and organisms with  
439 unknown physiological traits were assigned into "Uncategorized" group. Subglacial microbes  
440 accounted for 43 to 45 % of reads in year 0 and 5, and declined in older soils (year 50 and 113) to 18  
441 to 22%. The subglacial community was predominantly chemolithoautotrophic (A<sub>1</sub>). Typical soil  
442 bacteria (A<sub>2</sub> and H<sub>2</sub>) increased from low abundance (30% and 40% in years 0 and 5 respectively) to  
443 relatively high abundance (63 to 67%) of reads in years 50 and 113. Nitrogen fixing bacteria were  
444 prevalent in recently exposed soils (14% in year 0) but low in relative abundance in soils above 5  
445 years of age (4 to 6% in years 5, 50 and 113). In the freshly exposed soil (year 0), the microbial  
446 community was relatively evenly distributed between heterotrophs (43%) and autotrophs (44%). In  
447 developed soils, the relative abundance of heterotrophs increased (up to 74% of reads in years 50

Formatted: Font: Not Italic

Formatted: Font: Not Italic

Formatted: Font: Not Italic

Formatted: Font: Not Italic

Formatted: Font: Not Italic

Formatted: Font: Not Italic

Formatted: Font: Not Italic

Formatted: Font: Not Italic

Formatted: Font: Not Italic

Formatted: Font: Not Italic

Formatted: Font: Not Italic

Formatted: Font: Not Italic

Formatted: Font: Not Italic

Formatted: Font: Not Italic

Formatted: Font: Not Italic

448 and 113). Important to note is the fact that between 8 and 21% of the reads across all samples could  
449 not be classified.

450

### 451 3.2. Model Results

452 The model predicted an accumulation of autotrophic and heterotrophic biomass over 120 years (Fig.  
453 43a and 43b). Biomass and nutrient concentrations were initially extremely low (total biomass < 0.25  
454  $\mu\text{g C g}^{-1}$ , DIN < 4.0  $\mu\text{g N g}^{-1}$ , DIP < 3.0  $\mu\text{g P g}^{-1}$ ), and biological activity in initial soils was also low  
455 (Table 3). There was an order of magnitude increase in total microbial biomass in years 10 to 60.  
456 Nitrogen-fixing autotrophs ( $A_3$ ) and heterotrophs ( $H_3$ ), and soil heterotrophs ( $H_2$ ) experienced rapid  
457 growth during this period. Subglacial and soil autotrophs ( $A_{1-2}$ ) and subglacial heterotrophs ( $H_1$ )  
458 remained low. Bacterial production increased by roughly two orders of magnitude (Table 3). Organic  
459 carbon (labile and refractory) increased (Fig. 43c), whilst DIN and DIP concentrations increased by  
460 approximately an order of magnitude in the first 60 years (Fig. 43d). During the later stages of soil  
461 development (years 60 to 120), biomass increased rapidly due to the rapid growth of soil organisms  
462 ( $A_2$  and  $H_2$ ), which outcompeted nitrogen-fixers. The model showed a rapid exhaustion of labile  
463 organic carbon (years 50 to 100), while refractory carbon accumulated slowly. Nutrients (DIN and  
464 DIP) accumulated at a relatively constant rate. Microbial activity, including bacterial production,  
465 nitrogen fixation and DIN assimilation, was high relative to early stages (Table 3).

466

467 A carbon budget of fluxes through the substrate pool is presented in Fig. 54. Daily fluxes are  
468 presented in panels (a) for year 5, (b) for year 50 and (c) for year 113, and annual fluxes up to year  
469 120 are presented in (d). In recently exposed soils (5 years), allochthonous inputs were the only  
470 noticeable carbon flux, outweighing heterotrophic growth and respiration, and the contribution of  
471 substrate from necromass and exudates by over two orders of magnitude (Fig. 54a). Thus, the total  
472 change in carbon (black line) closely resembled allochthonous input. In the intermediate stages (Fig.  
473 54b), there was substantial depletion from the substrate pool due to heterotrophic activity.  
474 Heterotrophic growth (red line) was low despite high substrate consumption and respiration (orange  
475 line). In the late stages of soil development, the flux of microbial necromass was a significant  
476 contributor to the organic substrate pools (Fig. 54c). Carbon fluxes in mid to late stages of soil  
477 development were highly seasonal (Fig. 54b and 54c). Biotic fluxes (e.g. respiration) were up to six  
478 times higher during the summer (July to September) compared to the winter (November to April),  
479 however a base rate of heterotrophic respiration and turnover of microbial biomass was sustained  
480 over winter. Figure 4d shows that the contribution of microbial necromass rose steadily throughout the  
481 simulation (blue line), however was not sufficient to compensate the uptake of carbon substrate, thus  
482 leading to overall depletion between years 50 to 110 (black line). The contribution of exudates (green  
483 line) to substrate was minimal at all soil ages.

484

## 485 4. Discussion

### 486 4.1. Determination of parameters and model predictions

487 ~~The maximum microbial growth rate ( $I_{max}$ ) was determined by incorporation of  $^3\text{H}$ -leucine as 0.550~~  
488 ~~day<sup>-1</sup>(Bradley et al., 2015). This value is, to our knowledge, is the first measured rate of bacterial~~  
489 ~~growth from High Arctic soils, and falls within the lower end of the plausible range established in~~  
490 ~~Bradley et al. (2015) (0.24 – 4.80 day<sup>-1</sup>) for soil microbes from a range of laboratory and modelling~~  
491 ~~studies (Fig. 5a) (Frey et al., 2010; Ingwersen et al., 2008; Knapp et al., 1983; Zelenov et al., 2000;~~  
492 ~~Stapleton et al., 2005; Darrah, 1991; Blagodatsky et al., 1998; Vandeworff and Vorstraete, 1987;~~  
493 ~~Feerid and Yearsley, 2004; Toal et al., 2000; Scott et al., 1995). Figure 6 illustrates the influence of~~  
494 ~~the site-specific, laboratory-derived parameters on microbial biomass predictions. It compares the~~  
495 ~~range of predicted microbial biomass based on laboratory-determined parameters (yellow) to the~~  
496 ~~entire plausible parameter range (red; Bradley et al. (2015)). Predicted biomass with the average~~  
497 ~~laboratory-derived value is indicated by the black line. For  $I_{max}$ , predicted biomass with laboratory-~~  
498 ~~derived parameters (yellow shading) was towards the lower end of the plausible range (Fig. 6a)~~  
499 ~~because refined growth rates were significantly lower than the maximum values explored previously.~~  
500 ~~This was mostly due to a significant reduction in autotrophic biomass ( $A_{1-3}$ ). With high growth rates,~~  
501 ~~there was a sharp early increase in biomass (years 10 to 20) followed by slower growth phase (years~~  
502 ~~20 to 120). Model results with laboratory-derived growth rates showed that the exponential growth~~  
503 ~~phase occurred later (years 40 to 80) and was more prolonged, but total biomass was considerably~~  
504 ~~lower. There was a substantial reduction in the plausible range in predicted microbial biomass.~~

Field Code Changed

506 ~~The laboratory-derived  $Q_{10}$  for Midtre Lovénbreen was at the upper end of the plausible range~~  
507 ~~previously identified in Bradley et al. (2015) (Fig. 5b). There was a substantial reduction in the~~  
508 ~~plausible range in predicted microbial biomass (Fig. 6b) from the measured temperature sensitivity~~  
509 ~~( $Q_{10}$ ) (yellow) compared to the previous range (red). Soil microbial communities in Polar regions must~~  
510 ~~contend with extremely harsh environmental conditions such as cold temperatures, frequent freeze-~~  
511 ~~thaw cycles, low water availability, low nutrient availability, high exposure to ultraviolet radiation in the~~  
512 ~~summer, and prolonged periods of darkness in winter. These factors profoundly impact their~~  
513 ~~metabolism and survival strategies and ultimately shape the structure of the microbial community~~  
514 ~~(Cary et al., 2010). High  $Q_{10}$  values, as derived here, are typical of cold environments and cold~~  
515 ~~adapted organisms and this has been associated with the survival of biomass under prolonged~~  
516 ~~periods of harsh environmental conditions (Schipper et al., 2014). An investigation into the~~  
517 ~~metabolism of microbial communities in biological soils crusts in recently exposed soils from the East~~  
518 ~~Brøgger Glacier, approximately 6 km from the Midtre Lovénbreen catchment, also derived a high  $Q_{10}$~~   
519 ~~(3.1) (Yoshitake et al., 2010). The Midtre Lovénbreen catchment, in Svalbard, experiences a relatively~~  
520 ~~extreme Arctic climate. The high  $Q_{10}$  ultimately lowers the overall rate of biomass accumulation in~~  
521 ~~ultra-oligotrophic soils and a baseline population is maintained.~~

Formatted: Font: Italic

Formatted: Font: Italic, Subscript

523 ~~Measured BGE ( $Y_H$ ) was 0.06 (Fig. 5c). The low ~~measured BGE~~~~BGE calculated here (0.06)~~~~

524 suggested that a high proportion (94%) of substrate consumed by heterotrophs is **recycled**

525 **remineralized** (degrading organic substrate into DIC ( $\text{CO}_2$ ), DIN and DIP), with very little being

526 incorporated into biomass (6%). Low BGE encouraged the liberation and release of nutrients to the

527 soil and thus the overall growth response of the total microbial biomass was more rapid due to higher  
528 soil nutrient concentrations (Fig. 6c). However, due to the low BGE, there was a high rate of substrate  
529 degradation, and as such, labile substrate was rapidly depleted when heterotrophic biomass was high  
530 (Fig. 43c). Heterotrophic growth requires that a substantial amount of substrate is degraded – thus,  
531 although autotrophic production outweighed heterotrophic production at all stages of development  
532 (Fig. 43e), the soil was predicted by the model to be a net source of CO<sub>2</sub> to the atmosphere over the  
533 first 120 years of exposure (Fig. 43f). There are very few measurements of BGE in cold glaciated  
534 environments, however previous studies have suggested values as low as 0.0035 to 0.033 (Anesio et  
535 al., 2010; Hodson et al., 2007).

536 A major assumption of SHIMMER is that parameter values remain constant throughout the duration of  
537 the simulation. Empirical evidence suggests that parameters defined as fixed in SHIMMER (e.g. Q<sub>10</sub>)  
538 may be variable over time, however in SHIMMER, like many numerical modelling formulations,  
539 changing environmental (temperature, light) and geochemical (carbon substrate, available nitrogen,  
540 available phosphorus) conditions drive subsequent variability in microbial activity via mathematical  
541 formulations (e.g. Monod kinetics, see Bradley et al. (2015)) affixed to parameter values. A second  
542 major assumption is the assignment of measured rates to parameters for all microbial functional  
543 groups. Rather than taxonomic based classification, SHIMMER distinguishes and classifies microbial  
544 communities based on functional traits. These mathematical formulations assigned to, for example,  
545 microbial growth, are different between groups to represent distinct functional traits associated with  
546 that group. Whilst actual rates may be different between different organisms, for the level of model  
547 complexity and outputs required, a community measurement of those parameters is sufficient,  
548 particularly considering that the differences are accounted for in the mathematical formulation of  
549 SHIMMER (see Bradley et al. (2015)).

#### 551

#### 552 **4.2. Microbial biomass dynamics and community structure**

553 Measured microbial biomass in the initial soils of Midtre Lovénbreen (0.23 µg C g<sup>-1</sup>, 0 years) was very  
554 low compared to initial soils in other deglaciated forefields of equivalent ages in lower latitudes, for  
555 example in the Alps (4 µg C g<sup>-1</sup>) (Bernasconi et al., 2011; Tscherko et al., 2003) and Canada (6 µg C  
556 g<sup>-1</sup>) (Insam and Haselwandter, 1989). However, our microbial biomass values are more similar to  
557 other recently deglaciated soils in Antarctica (Ecology Glacier - 0.88 µg C g<sup>-1</sup>) (Zdanowski et al.,  
558 2013). Low biomass is possibly a result of the harsh, ultra-oligotrophic and nutrient limiting  
559 environment of the High Arctic and Antarctica, where low temperature and longer winters limit the  
560 summer growth phase, especially compared to an Alpine system (Tscherko et al., 2003; Bernasconi  
561 et al., 2011).

562

563 The initial microbial community structure in our samples was predominantly autotrophic (74.5%). In  
564 the years following exposure, we observed an increase in autotrophs and heterotrophs with soil age  
565 (Table 2), presumably due to the establishment and growth of stable soil microbial communities  
566 (Schulz et al., 2013; Bradley et al., 2014). Both the observations and modelling results suggested that

Field Code Changed

Formatted: Font: 10 pt

Formatted: Font color: Auto

Formatted: Font: 10 pt



567 there was no substantial increase in heterotrophic biomass during the initial and early-intermediate  
568 stages of soil development (years 0 to 40), which was then followed by a growth phase whereby  
569 biomass increased by roughly an order of magnitude. Overall, the model and the microscopy data  
570 were in good agreement accounting for the limitations in both techniques, spatial heterogeneity, and  
571 the oscillations in biomass arising from seasonality (Fig. 7). SHIMMER predicted that low initial  
572 microbial populations have the potential to considerably increase in population density during several  
573 decades of soil development. This data thus supports the hypothesis that the observed increase in  
574 microbial biomass with soil age is a consequence of *in situ* growth and activity. The pattern of  
575 microbial abundance observed in the Midtre Lovénbreen forefield broadly resembles that of other  
576 glacier forefields worldwide (see Bradley et al. (2014)). For example, data from the Rootmoos Ferner  
577 (Austria) (Insam and Haselwandter, 1989), Athabasca (Canada) (Insam and Haselwandter, 1989),  
578 Damma (Switzerland) (Bernasconi et al., 2011; Schulz et al., 2013) and Puca (Peru) (Schmidt et al.,  
579 2008), glacier forefields find increased microbial biomass and activity over decades to centuries of soil  
580 development following exposure.  
581 The initial microbial community structure in our samples was predominantly autotrophic (74.5%). In  
582 the years following exposure, we observed an increase in autotrophs and heterotrophs with soil age  
583 (Table 3), presumably due to the establishment and growth of stable soil microbial communities  
584 (Schulz et al., 2013; Bradley et al., 2014). Both the observations and modelling results suggested that  
585 there was no substantial increase in heterotrophic biomass during the initial and early-intermediate  
586 stages of soil development (years 0 to 40), which was then followed by a growth phase whereby  
587 biomass increased by roughly an order of magnitude. Overall, the model and the microscopy data  
588 were in good agreement accounting for the limitations in both techniques, spatial heterogeneity, and  
589 the oscillations in biomass arising from seasonality. The pattern of microbial abundance observed in  
590 the Midtre Lovénbreen forefield broadly resembles that of other glacier forefields worldwide (Bradley et  
591 al. (2014) (Insam and Haselwandter, 1989; Bernasconi et al., 2011; Schulz et al., 2013) (Insam and  
592 Haselwandter, 1989; Bernasconi et al., 2011; Schulz et al., 2013; Schmidt et al., 2008)  
593  
594 The genomic data indicated that subglacial microbes are dominant in recently exposed soils, in  
595 agreement with model results (Fig. 8). The community structure in year 5 was heavily dominated by  
596 chemolithoautotrophs (A<sub>1</sub>), which reflected findings from previous studies whereby  
597 chemolithoautotrophic bacteria contribute to the oxidation of FeS<sub>2</sub> in proglacial moraines in Midtre  
598 Lovénbreen (Borin et al., 2010; Mapelli et al., 2011). These processes are also commonly described  
599 in other subglacial habitats (Boyd et al., 2014; Hamilton et al., 2013). Based on 16S data, the  
600 subglacial community declined in relative abundance with soil age. This finding was also reflected in  
601 the model in years 50 and 113. As the age of the soil progressed, there was typically greater  
602 abundance of microbes representing typical soil bacteria (groups A<sub>2</sub> and H<sub>2</sub>) in the 16S data and the  
603 model, thus the relative abundance of subglacial microbes decreased.  
604  
605 Microscopic analyses indicated low total biomass in recently exposed soils (up to 1.7 µg C g<sup>-1</sup> in soil  
606 exposed for 50 years) that was comprised predominantly of autotrophic bacteria. Model simulations

Formatted: Font color: Auto

Formatted: Font: 10 pt

Formatted: Font: 10 pt

Formatted: Font: 10 pt

Formatted: Font: 10 pt

Formatted: Font: 10 pt

Formatted: Font: 10 pt

Formatted: Font: 10 pt

Formatted: Font: 10 pt

Formatted: Font: 10 pt

Field Code Changed

Field Code Changed

Field Code Changed

Field Code Changed

Formatted: Line spacing: 1.5 lines



607 agreed well with microscopy derived data. Overall, the 16S data, when categorised into functional  
608 groups as defined by the model, agreed well with the microscopy and model output in the very early  
609 stages of soil development. However, in later stages of soil development (50 years and older),  
610 microscopy and modelling suggested a continuation of predominantly autotrophic soil microbial  
611 communities whereas 16S sequence data notably indicated a predominantly heterotrophic  
612 community. With extremely low biomass, cell counts derived from microscopy, as well as  
613 representation of relative abundance by 16S extraction and amplification, can be largely skewed by  
614 relatively small changes in the soil microbial community. Furthermore, the comparative difficulty to  
615 lyse autotrophic bacteria (such as some groups of cyanobacteria) from an environmental sample  
616 compared to heterotrophic bacteria, and thus successfully amplify the 16S gene during the PCR  
617 process, may skew 16S sequence data in favour of heterotrophic sequence reads. Additionally,  
618 SHIMMER is an ambitious model in that it attempts to simulate, predict and constrain multiple  
619 functional types of bacteria species in a numerical framework. Numerical models containing multiple  
620 species or multiple microbial functional groups are often extremely challenging to constrain (Servedio  
621 et al., 2014; Hellweger and Bucci, 2009; Jessup et al., 2004; Larsen et al., 2012), and as such, the  
622 majority of microbial soil models often only resolve one or two living biomass pool that represents the  
623 bulk activity and function of the entire community (see e.g. Manzoni et al. (2004), Manzoni and  
624 Porporato (2007), Blagodatsky and Richter (1998), Ingwersen et al. (2008), Wang et al. (2014) and  
625 others). Our rationale for resolving six distinct functional groups was to quantitatively assess, using  
626 modelling, the relative importance and role of each functional group at different stages of soil  
627 development. Regardless of discrepancies in older soils (over 50 years since exposure), both the 16S  
628 and microscopy data indicated that there was a mixed community of autotrophs and heterotrophs in  
629 soils of all ages, which was supported by modelling, since no functional groups were extirpated over  
630 simulations representing 120 years of soil development. Thus, SHIMMER is able to capture the  
631 diversity of the sample over 120 years of soil development, but the detailed community composition  
632 requires further investigation.

633 ▲  
634 Nitrogen-fixing bacteria were prevalent in recently exposed soils but declined in relative abundance  
635 with soil age. By fixing N<sub>2</sub> instead of assimilating DIN, the model predicted that nitrogen-fixers were  
636 able to grow rapidly in the early stages relative to other organisms (Fig. 4a, 4b). The model prediction  
637 supports findings by previous studies demonstrating the importance of nitrogen fixation in Alpine (Duc  
638 et al., 2009; Schmidt et al., 2008) and Antarctic (Strauss et al., 2012) glacier forefields and other High-  
639 Arctic (Svalbard, Greenland) glacial ecosystems (Telling et al., 2011; Telling et al., 2012). However,  
640 there was poor agreement on the relative abundance of nitrogen-fixers between the model and the  
641 16S data in the later stages of soil development (years 50 to 120), particularly between autotrophs  
642 and heterotrophs. The model over-predicted the relative abundance of nitrogen-fixing organisms (Fig.  
643 8). The majority of the biomass of the autotrophic nitrogen-fixers was composed of sequences  
644 belonging to the cyanobacterium from the genus *Nostoc*. *Nostoc* forms macroscopically visible  
645 colonies that grow on the surface of the soils. Its distribution in the Arctic soils is thus extremely  
646 patchy and therefore, part of the discrepancy between the 16S data and the model regarding the

Formatted: Font: Not Italic

647 relative distribution of the A<sub>3</sub> group in the older soils could be due to under-sampling of the *Nostoc*  
648 colonies as a consequence of a random sampling approach. Furthermore, allochthonous inputs of  
649 nitrogen to the Arctic (e.g. aerial deposition (Geng et al., 2014)) strongly affect the productivity of  
650 microbial ecosystems and the requirement of nitrogen fixation for microbes (Bjorkman et al., 2013;  
651 Kuhnel et al., 2013; Kuhnel et al., 2011; Hodson et al., 2010; Telling et al., 2012; Galloway et al.,  
652 2008). Thus, uncertainty in the allochthonous availability of nitrogen strongly affects nitrogen fixation  
653 rates. In attempting to replicate a qualitative understanding of the nitrogen cycle in a quantitative  
654 mathematical modelling framework, the predicted importance of nitrogen-fixing organisms may be  
655 over-estimated. The poor agreement in the relative abundance of nitrogen-fixers between the model  
656 and the 16S data indicates an incomplete understanding of allochthonous versus autochthonous  
657 nutrient availability. Allochthonous nutrient availability is a known source of uncertainty (Bradley et al.,  
658 2014; Schulz et al., 2013; Schmidt et al., 2008), and addressing this concern is the subject of future  
659 work.

660  
661 16S data is an exciting resource of information that is rarely (or never) used to test models. However,  
662 the environment (difficulty to extract DNA), the presentation (percentages of low concentration and  
663 thus easy to shift relative abundance) and model uncertainties make comparisons challenging. In  
664 making this first attempt at comparison of model output to 16S data, we hope to spark discussion and  
665 further development of approaches that have similar objectives in order to improve future model  
666 performance.

667 Microscopy and modelling indicated a predominantly autotrophic community, however 16S data  
668 indicated the contrary – especially in the later stages of soil development. Nevertheless, both the 16S  
669 and microscopy data indicated that there was a mixed community of autotrophs and heterotrophs in  
670 soils of all ages, which was supported by modelling, since no functional groups were extirpated over  
671 simulations representing 120 years of soil development.

672  
673 Nitrogen-fixing bacteria were prevalent in recently exposed soils but declined in relative abundance  
674 with soil age. By fixing N<sub>2</sub> instead of assimilating DIN, the model predicted that nitrogen-fixers were  
675 able to grow rapidly in the early stages relative to other organisms (Fig. 3a and 3b). The model  
676 prediction supports findings by previous studies demonstrating the importance of nitrogen fixation in  
677 (Duc et al., 2009; Schmidt et al., 2008; Strauss et al., 2012) glacier forefields (Duc et al., 2009;  
678 Schmidt et al., 2008; Strauss et al., 2012) and other glacial ecosystems (Telling et al., 2011; Telling et  
679 al., 2012). However, there was poor agreement on the relative abundance of nitrogen fixers between  
680 the model and the 16S data in the later stages of soil development (years 50 to 120). The model over-  
681 predicted the relative abundance of nitrogen fixing organisms (Fig. 8). The majority of the biomass of  
682 the autotrophic nitrogen fixers was composed of sequences belonging to the cyanobacterium from the  
683 genus *Nostoc*. *Nostoc* forms macroscopically visible colonies that grow on the surface of the soils. Its  
684 distribution in the Arctic soils is thus extremely patchy and therefore part of the discrepancy between  
685 the 16S data and the model regarding the relative distribution of the A<sub>3</sub> group in the older soils could  
686 be due to under-sampling of the *Nostoc* colonies. Allochthonous inputs of nitrogen to the Arctic (e.g.

687 aerial deposition (Geng et al., 2014)) strongly affect the productivity of microbial ecosystems and the  
688 requirement of nitrogen fixation for microbes (Bjorkman et al., 2013; Kuhnelt et al., 2013; Kuhnelt et al.,  
689 2011; Hodson et al., 2010; Telling et al., 2012; Galloway et al., 2008). Thus, uncertainty in the  
690 allochthonous availability of nitrogen strongly affects nitrogen fixation rates. In attempting to replicate  
691 a qualitative understanding of the nitrogen cycle in a quantitative mathematical modelling framework,  
692 the predicted importance of nitrogen-fixing organisms may be over-estimated. The poor agreement in  
693 the relative abundance of nitrogen-fixers between the model and the 16S data indicates an  
694 incomplete understanding of allochthonous versus autochthonous nutrient availability. Allochthonous  
695 nutrient availability is a known source of uncertainty (Bradley et al., 2014; Schulz et al., 2013; Schmidt  
696 et al., 2008), and addressing this concern is the subject of future work.

### 698 4.3. Net ecosystem metabolism and carbon budget

699 Allochthonous carbon inputs were the most significant contributor to recently exposed soils (e.g. year  
700 5), since the total change in substrate closely followed this flux (Fig. 5). In older soils (year 113), biotic  
701 fluxes were substantially higher, and microbial necromass contributed equally as a source of organic  
702 substrate compared to allochthonous deposition. In the older soils, heterotrophic growth and  
703 respiration caused substantial consumption and thus depletion of available carbon stocks. This  
704 evidence thus supports the hypothesis that carbon fluxes in very recently exposed soils are low and  
705 are dominated by abiotic processes (i.e. allochthonous deposition), whereas biotic processes (such  
706 as microbial growth, respiration and cell death) play a greater role in developed soils with increased  
707 microbial abundance and activity. These findings for the Midtre Lovénbreen glacier in the High-Arctic,  
708 are similar to what has been observed based on empirical evidence from Alpine settings (at the  
709 Damma Glacier, Switzerland (Smittenberg et al., 2012; Guelland et al., 2013)),

712 The seasonality of carbon fluxes predicted by the model (Fig. 5.4b and 5.4c) related to the high  
713 measured  $Q_{10}$  values. High seasonal variation in biotic fluxes and rates is typical of cryospheric soil  
714 ecosystems (Schostag et al., 2015) including Alpine glacier forefield soils (Lazzaro et al., 2012;  
715 Lazzaro et al., 2015). However, microbial activity has been shown to persist during winter under  
716 insulating layers of snow and in sub-zero temperatures (Zhang et al., 2014). Modelling also predicted  
717 sustained organic substrate degradation, microbial turnover and net heterotrophy during the winter  
718 (Fig. 5.4b and 5.4c), as documented in other glacier forefield studies from an Alpine setting (Guelland  
719 et al., 2013b), at a low rate.

721 The low measured BGE has three important consequences. Firstly, low BGE suggests that a large  
722 pool of substrate is required to support heterotrophic growth. Low-efficiency heterotrophic growth lead  
723 to the rapid depletion of substrate; therefore high allochthonous inputs were required to maintain a  
724 sizeable pool. In older soils (years 80 to 120), increased inputs from microbial necromass (blue line,  
725 Fig. 5.4d) sustained substrate supply to heterotrophs. The sources of allochthonous carbon substrate  
726 to the glacier forefield include meltwater inputs derived from the supraglacial and subglacial

Formatted: Font: 10 pt

Formatted: Font: 10 pt

Formatted: Font: 10 pt

Formatted: Font: 10 pt

Formatted: Font: 10 pt

Formatted: Font: 10 pt

Formatted: Font: 10 pt

Formatted: Font: 10 pt

Formatted: Font: 10 pt

Formatted: Font: Bold

727 ecosystems (Stibal et al., 2008; Hodson et al., 2005; Mindl et al., 2007), snow algae (which are known  
728 to be prolific primary colonizers and producers in High Arctic snow packs (Lutz et al., 2015; Lutz et al.,  
729 2014), atmospheric deposition (Kuhnel et al., 2013) and ornithogenic deposition (e.g. fecal matter of  
730 birds and animals) (Jakubas et al., 2008; Ziolk and Melke, 2014; Luoto et al., 2015; Michelutti et al.,  
731 2009; Michelutti et al., 2011; Moe et al., 2009). Microbial dynamics are moderately sensitive to  
732 external allochthonous inputs of substrate (Bradley et al., 2015), and addressing the uncertainty  
733 associated with this flux is an important question to address in future research.

734  
735 Secondly, low BGE causes a net efflux of CO<sub>2</sub> over the first 120 years of soil development despite  
736 high autotrophic production (Fig. 43e and 43f). Recent literature has explored the carbon dynamics of  
737 glacier forefield ecosystems, finding highly variable soil respiration rates (Bekku et al., 2004; Schulz et  
738 al., 2013; Guelland et al., 2013a). Future studies should focus on quantifying carbon and nutrient  
739 transformations and the potential for forefield systems to impact global biogeochemical cycles in  
740 response to future climate change (Smittenberg et al., 2012) and in the context of large-scale ice  
741 retreat.

742  
743 Thirdly, high rates of substrate degradation encouraged by low BGE were responsible for rapid  
744 nutrient release~~Thirdly, high rates of substrate degradation encouraged by low BGE were responsible~~  
745 ~~for rapid nutrient release.~~ Modelling suggested that microbial growth was strongly inhibited by low  
746 nutrient availability in initial soils (4 µg N g<sup>-1</sup>, 2 to 10 µg P g<sup>-1</sup>) (Fig. 43d). This is consistent with  
747 findings from the Hailuoguo Glacier (Gongga Shan, China) and Damma Glacier (Switzerland)  
748 (Prietz et al., 2013). Low BGE is predicted by the model to have a very important role in  
749 encouraging the release of nutrients from organic material more rapidly, thereby increasing total  
750 bacterial production in the intermediate stages of soil development. Increased nutrient availability with  
751 increased heterotrophic biomass is consistent with recent observations from glacier forefields (Bekku  
752 et al., 2004; Schulz et al., 2013; Schmidt et al., 2008).

753

## 754 5. Conclusions

755 We used laboratory-based mesocosm experiments to measure three key model parameters:  
756 maximum microbial growth rate ( $I_{max}$ ) (by incorporation of <sup>3</sup>H-leucine), BGE (Y) (by measuring  
757 respiration rates) and the temperature response ( $Q_{10}$ ) (by measuring rates at different ambient  
758 temperatures). Laboratory-derived parameters were comparable with previous estimations, and  
759 refined model predictions by narrowing the range of model output over nominal environmental  
760 conditions, thus increasing confidence in model predictions. Our results demonstrated that in situ  
761 microbial growth lead to the overall accumulation of microbial biomass in the Midtre Lovénbreen  
762 forefield during the first century of soil development following exposure. Furthermore, carbon fluxes  
763 increased in older soils due to elevated biotic (microbial) activity. Microbial dynamics at the initial  
764 stages of soil development in glacial forefields do not contribute to significant accumulation of organic  
765 carbon due to the very low growth efficiency of the microbial community, resulting in a net efflux of  
766 CO<sub>2</sub> from those habitats. However, the low bacterial growth efficiency in glacial forefields is also

Formatted: Font: Not Italic

Formatted: Font: Italic

767 responsible for high rates of nutrient ~~recycling~~ remineralization that most probably ~~have~~ has an  
768 important role on the establishment of plants at older ages. The relative importance of allochthonous  
769 versus autochthonous substrate and nutrients is the focus of future research.

770  
771 Much of the extreme ice-free regions in Antarctica are characterized by a complete absence of higher  
772 order plants. However even these environments contain diverse microbial populations and extremely  
773 low but detectable levels of organic carbon (Cowan et al., 2014), making these environments suitable  
774 cases for modelling using SHIMMER. This exercise shows how an integrated model-data approach  
775 can improve understanding and predictions of microbial dynamics in forefield soils and disentangle  
776 complex process interactions to ascertain the relative importance of each process independently. This  
777 would, for annual budgets, be extremely challenging with a purely empirical approach. Nevertheless,  
778 more clarity and data are needed in tracing the dynamics and interactions of these carbon pools to  
779 improve confidence and validate model simulations~~This exercise shows how an integrated model-~~  
780 ~~data approach can improve understanding and predictions of microbial dynamics in forefield soils and~~  
781 ~~disentangle complex processes interactions to ascertain the relative importance of each process~~  
782 ~~independently.~~ This combined approach explored detailed microbial and biogeochemical dynamics of  
783 soil development with the view to obtaining a more holistic picture of soil development in a warmer  
784 and increasingly ice-free future world.

#### 785 786 **Acknowledgements**

787 We thank Siegrid Debatin, Marion Maturilli, and Julia Boike (AWI) for support in acquiring  
788 meteorological and radiation data, Simon Cobb and James Williams (University of Bristol) for  
789 laboratory assistance, and Nicholas Cox and James Wake for assistance in the field and use of the  
790 UK Station Arctic Research base in Ny-Ålesund. We also thank the two anonymous referees who  
791 provided valuable comments on the manuscript. This research was supported by NERC grant no.  
792 NE/J02399X/1 to A. M. Anesio. S. Arndt acknowledges support from NERC grant no. NE/I021322/1.

#### 793 794 795 **References**

796 ACIA: Arctic Climate Impacts Assessment, Cambridge University Press, Cambridge, 1042,  
797 2005.  
798 Alves, R. J. E., Wanek, W., Zappe, A., Richter, A., Svenning, M. M., Schleper, C., and Ulrich, T.:  
799 Nitrification rates in Arctic soils are associated with functionally distinct populations of  
800 ammonia-oxidizing archaea, *Isme J*, 7, 1620-1631, 10.1038/ismej.2013.35, 2013.  
801 Anderson, S. P., Drever, J. I., Frost, C. D., and Holden, P.: Chemical weathering in the  
802 foreland of a retreating glacier, *Geochim Cosmochim Ac*, 64, 1173-1189, Doi 10.1016/S0016-  
803 7037(99)00358-0, 2000.  
804 Anesio, A. M., Hodson, A. J., Fritz, A., Psenner, R., and Sattler, B.: High microbial activity on  
805 glaciers: importance to the global carbon cycle, *Global Change Biol*, 15, 955-960, DOI  
806 10.1111/j.1365-2486.2008.01758.x, 2009.

807 Anesio, A. M., Sattler, B., Foreman, C., Telling, J., Hodson, A., Tranter, M., and Psenner, R.:  
808 Carbon fluxes through bacterial communities on glacier surfaces, *Ann Glaciol*, 51, 32-40,  
809 2010.

810 Bekku, Y. S., Nakatsubo, T., Kume, A., and Koizumi, H.: Soil microbial biomass, respiration  
811 rate, and temperature dependence on a successional glacier foreland in Ny-Alesund,  
812 Svalbard, *Arct Antarct Alp Res*, 36, 395-399, 2004.

813 Bernasconi, S. M., Bauder, A., Bourdon, B., Brunner, I., Bunemann, E., Christl, I., Derungs, N.,  
814 Edwards, P., Farinotti, D., Frey, B., Frossard, E., Furrer, G., Gierga, M., Goransson, H.,  
815 Gulland, K., Hagedorn, F., Hajdas, I., Hindshaw, R., Ivy-Ochs, S., Jansa, J., Jonas, T., Kiczka, M.,  
816 Kretzschmar, R., Lemarchand, E., Luster, J., Magnusson, J., Mitchell, E. A. D., Venterink, H.  
817 O., Plotze, M., Reynolds, B., Smittenberg, R. H., Stahli, M., Tamburini, F., Tipper, E. T.,  
818 Wacker, L., Welc, M., Wiederhold, J. G., Zeyer, J., Zimmermann, S., and Zumsteg, A.:  
819 Chemical and Biological Gradients along the Damma Glacier Soil Chronosequence,  
820 Switzerland, *Vadose Zone J*, 10, 867-883, Doi 10.2136/Vzj2010.0129, 2011.

821 Berner, R. A., Lasaga, A. C., and Garrels, R. M.: The Carbonate-Silicate Geochemical Cycle  
822 and Its Effect on Atmospheric Carbon-Dioxide over the Past 100 Million Years, *Am J Sci*, 283,  
823 641-683, 1983.

824 Billings, W. D.: Carbon Balance of Alaskan Tundra and Taiga Ecosystems - Past, Present and  
825 Future, *Quaternary Sci Rev*, 6, 165-177, Doi 10.1016/S0277-3791(00)90007-6, 1987.

826 Bjorkman, M. P., Kuhnel, R., Partridge, D. G., Roberts, T. J., Aas, W., Mazzola, M., Viola, A.,  
827 Hodson, A., Strom, J., and Isaksson, E.: Nitrate dry deposition in Svalbard, *Tellus B*, 65, Art  
828 19071  
829 Doi 10.3402/Tellusb.V65i0.19071, 2013.

830 Blagodatsky, S. A., and Richter, O.: Microbial growth in soil and nitrogen turnover: A  
831 theoretical model considering the activity state of microorganisms, *Soil Biol Biochem*, 30,  
832 1743-1755, Doi 10.1016/S0038-0717(98)00028-5, 1998.

833 Blagodatsky, S. A., Yevdokimov, I. V., Larionova, A. A., and Richter, J.: Microbial growth in  
834 soil and nitrogen turnover: Model calibration with laboratory data, *Soil Biol Biochem*, 30,  
835 1757-1764, Doi 10.1016/S0038-0717(98)00029-7, 1998.

836 Borin, S., Ventura, S., Tambone, F., Mapelli, F., Schubotz, F., Brusetti, L., Scaglia, B., D'Acqui,  
837 L. P., Solheim, B., Turicchia, S., Marasco, R., Hinrichs, K. U., Baldi, F., Adani, F., and  
838 Daffonchio, D.: Rock weathering creates oases of life in a High Arctic desert, *Environ*  
839 *Microbiol*, 12, 293-303, DOI 10.1111/j.1462-2920.2009.02059.x, 2010.

840 Boyd, E. S., Hamilton, T. L., Havig, J. R., Skidmore, M. L., and Shock, E. L.: Chemolithotrophic  
841 Primary Production in a Subglacial Ecosystem, *Appl Environ Microb*, 80, 6146-6153,  
842 10.1128/Aem.01956-14, 2014.

843 Bradley, J. A., Singarayer, J. S., and Anesio, A. M.: Microbial community dynamics in the  
844 forefield of glaciers, *Proceedings. Biological sciences / The Royal Society*, 281, 2793-2802,  
845 10.1098/rspb.2014.0882, 2014.

846 Bradley, J. A., Anesio, A. M., Singarayer, J. S., Heath, M. R., and Arndt, S.: SHIMMER (1.0): a  
847 novel mathematical model for microbial and biogeochemical dynamics in glacier forefield  
848 ecosystems, *Geosci. Model Dev.*, 8, 3441-3470, 10.5194/gmd-8-3441-2015, 2015.

849 Bradley, J. A., Anesio, A., and Arndt, S.: Bridging the divide: a model-data approach to Polar  
850 & Alpine Microbiology, *Fems Microbiol Ecol*, 92, 10.1093/femsec/fiw015, 2016.

851 Bratbak, G., and Dundas, I.: Bacterial Dry-Matter Content and Biomass Estimations, *Appl*  
852 *Environ Microb*, 48, 755-757, 1984.

853 Brown, S. P., and Jumpponen, A.: Contrasting primary successional trajectories of fungi and  
854 bacteria in retreating glacier soils, *Mol Ecol*, 23, 481-497, Doi 10.1111/Mec.12487, 2014.

855 Caporaso, J. G., Kuczynski, J., Stombaugh, J., Bittinger, K., Bushman, F. D., Costello, E. K.,  
856 Fierer, N., Pena, A. G., Goodrich, J. K., Gordon, J. I., Huttley, G. A., Kelley, S. T., Knights, D.,  
857 Koenig, J. E., Ley, R. E., Lozupone, C. A., McDonald, D., Muegge, B. D., Pirrung, M., Reeder, J.,  
858 Sevinsky, J. R., Tumbaugh, P. J., Walters, W. A., Widmann, J., Yatsunencko, T., Zaneveld, J.,  
859 and Knight, R.: QIIME allows analysis of high-throughput community sequencing data, *Nat*  
860 *Methods*, 7, 335-336, 10.1038/nmeth.f.303, 2010.

861 Cary, S. C., McDonald, I. R., Barrett, J. E., and Cowan, D. A.: On the rocks: the microbiology of  
862 Antarctic Dry Valley soils, *Nat Rev Microbiol*, 8, 129-138, 10.1038/nrmicro2281, 2010.

863 Cowan, D. A., Makhalyane, T. P., Dennis, P. G., and Hopkins, D. W.: Microbial ecology and  
864 biogeochemistry of continental Antarctic soils, *Frontiers in microbiology*, 5, Artn 154  
865 Doi 10.3389/Fmicb.2014.00154, 2014.

866 Darrah, P. R.: Models of the Rhizosphere .1. Microbial-Population Dynamics around a Root  
867 Releasing Soluble and Insoluble Carbon, *Plant Soil*, 133, 187-199, Doi 10.1007/Bf00009191,  
868 1991.

869 Dessert, C., Dupre, B., Gaillardet, J., Francois, L. M., and Allegre, C. J.: Basalt weathering laws  
870 and the impact of basalt weathering on the global carbon cycle, *Chem Geol*, 202, 257-273,  
871 DOI 10.1016/j.chemgeo.2002.10.001, 2003.

872 Duc, L., Noll, M., Meier, B. E., Burgmann, H., and Zeyer, J.: High Diversity of Diazotrophs in  
873 the Forefield of a Receding Alpine Glacier, *Microbial Ecol*, 57, 179-190, DOI 10.1007/s00248-  
874 008-9408-5, 2009.

875 Dyurgerov, M. B., and Meier, M. F.: Twentieth century climate change: Evidence from small  
876 glaciers, *P Natl Acad Sci USA*, 97, 1406-1411, DOI 10.1073/pnas.97.4.1406, 2000.

877 Edgar, R. C., Haas, B. J., Clemente, J. C., Quince, C., and Knight, R.: UCHIME improves  
878 sensitivity and speed of chimera detection, *Bioinformatics*, 27, 2194-2200,  
879 10.1093/bioinformatics/btr381, 2011.

880 Ensign, K. L., Webb, E. A., and Longstaffe, F. J.: Microenvironmental and seasonal variations  
881 in soil water content of the unsaturated zone of a sand dune system at Pinery Provincial  
882 Park, Ontario, Canada, *Geoderma*, 136, 788-802, DOI 10.1016/j.geoderma.2006.06.009,  
883 2006.

884 Esperschütz, J., Perez-de-Mora, A., Schreiner, K., Welzl, G., Buegger, F., Zeyer, J., Hagedorn,  
885 F., Munch, J. C., and Schloter, M.: Microbial food web dynamics along a soil chronosequence  
886 of a glacier forefield, *Biogeosciences*, 8, 3283-3294, DOI 10.5194/bg-8-3283-2011, 2011.

887 Filippelli, G. M.: The global phosphorus cycle, *Rev Mineral Geochem*, 48, 391-425, DOI  
888 10.2138/rmg.2002.48.10, 2002.

889 Fleming, K. M., Dowdeswell, J. A., and Oerlemans, J.: Modelling the mass balance of  
890 northwest Spitsbergen glaciers and responses to climate change, *Annals of Glaciology*, Vol  
891 24, 1997, 24, 203-210, 1997.

892 Foeroid, B., and Yearsley, J. M.: Modelling the impact of microbial grazers on soluble  
893 rhizodeposit turnover, *Plant Soil*, 267, 329-342, DOI 10.1007/s11104-005-0139-9, 2004.

894 Follmi, K. B., Hosein, R., Arn, K., and Steinmann, P.: Weathering and the mobility of  
895 phosphorus in the catchments and forefields of the Rhone and Oberaar glaciers, central  
896 Switzerland: Implications for the global phosphorus cycle on glacial-interglacial timescales,  
897 *Geochim Cosmochim Acta*, 73, 2252-2282, DOI 10.1016/j.gca.2009.01.017, 2009.

898 Fountain, A. G., Nylén, T. H., Tranter, M., and Bagshaw, E.: Temporal variations in physical  
899 and chemical features of cryoconite holes on Canada Glacier, McMurdo Dry Valleys,  
900 Antarctica, *J Geophys Res-Biogeophys*, 113, Artn G01s92  
901 Doi 10.1029/2007jg000430, 2008.

902 Frey, B., Rieder, S. R., Brunner, I., Plotze, M., Koetzsch, S., Lapanje, A., Brandl, H., and Furrer,  
903 G.: Weathering-Associated Bacteria from the Damma Glacier Forefield: Physiological  
904 Capabilities and Impact on Granite Dissolution, *Appl Environ Microb*, 76, 4788-4796, Doi  
905 10.1128/Aem.00657-10, 2010.

906 Frey, B., Buhler, L., Schmutz, S., Zumsteg, A., and Furrer, G.: Molecular characterization of  
907 phototrophic microorganisms in the forefield of a receding glacier in the Swiss Alps, *Environ*  
908 *Res Lett*, 8, Artn 015033  
909 Doi 10.1088/1748-9326/8/1/015033, 2013.

910 Galloway, J. N., Townsend, A. R., Erismann, J. W., Bekunda, M., Cai, Z. C., Freney, J. R.,  
911 Martinelli, L. A., Seitzinger, S. P., and Sutton, M. A.: Transformation of the nitrogen cycle:  
912 Recent trends, questions, and potential solutions, *Science*, 320, 889-892,  
913 10.1126/science.1136674, 2008.

914 Geng, L., Alexander, B., Cole-Dai, J., Steig, E. J., Savarino, J., Sofen, E. D., and Schauer, A. J.:  
915 Nitrogen isotopes in ice core nitrate linked to anthropogenic atmospheric acidity change, *P*  
916 *Natl Acad Sci USA*, 111, 5808-5812, 10.1073/pnas.1319441111, 2014.

917 Goransson, H., Venterink, H. O., and Baath, E.: Soil bacterial growth and nutrient limitation  
918 along a chronosequence from a glacier forefield, *Soil Biol Biochem*, 43, 1333-1340, DOI  
919 10.1016/j.soilbio.2011.03.006, 2011.

920 Goulden, M. L., Wofsy, S. C., Harden, J. W., Trumbore, S. E., Crill, P. M., Gower, S. T., Fries, T.,  
921 Daube, B. C., Fan, S. M., Sutton, D. J., Bazzaz, A., and Munger, J. W.: Sensitivity of boreal  
922 forest carbon balance to soil thaw, *Science*, 279, 214-217, DOI  
923 10.1126/science.279.5348.214, 1998.

924 Guelland, K., Esperschütz, J., Bornhauser, D., Bernasconi, S. M., Kretschmar, R., and  
925 Hagedorn, F.: Mineralisation and leaching of C from C-13 labelled plant litter along an initial  
926 soil chronosequence of a glacier forefield, *Soil Biol Biochem*, 57, 237-247, DOI  
927 10.1016/j.soilbio.2012.07.002, 2013a.

928 Guelland, K., Hagedorn, F., Smittenberg, R. H., Goransson, H., Bernasconi, S. M., Hajdas, I.,  
929 and Kretschmar, R.: Evolution of carbon fluxes during initial soil formation along the  
930 forefield of Damma glacier, Switzerland, *Biogeochemistry*, 113, 545-561, DOI  
931 10.1007/s10533-012-9785-1, 2013b.

932 Hamilton, T. L., Peters, J. W., Skidmore, M. L., and Boyd, E. S.: Molecular evidence for an  
933 active endogenous microbiome beneath glacial ice, *Isme J*, 7, 1402-1412,  
934 10.1038/ismej.2013.31, 2013.

935 Hellweger, F. L., and Bucci, V.: A bunch of tiny individuals-Individual-based modeling for  
936 microbes, *Ecol Model*, 220, 8-22, DOI 10.1016/j.ecolmodel.2008.09.004, 2009.

937 Hodkinson, I. D., Coulson, S. J., and Webb, N. R.: Community assembly along proglacial  
938 chronosequences in the high Arctic: vegetation and soil development in north-west  
939 Svalbard, *J Ecol*, 91, 651-663, DOI 10.1046/j.1365-2745.2003.00786.x, 2003.

940 Hodson, A., Anesio, A. M., Ng, F., Watson, R., Quirk, J., Irvine-Fynn, T., Dye, A., Clark, C.,  
941 McCloy, P., Kohler, J., and Sattler, B.: A glacier respire: Quantifying the distribution and  
942 respiration CO<sub>2</sub> flux of cryoconite across an entire Arctic supraglacial ecosystem, *J Geophys*  
943 *Res-Biogeophys*, 112, Artn G04s36  
944 Doi 10.1029/2007jg000452, 2007.



945 Hodson, A., Roberts, T. J., Engvall, A. C., Holmen, K., and Mumford, P.: Glacier ecosystem  
946 response to episodic nitrogen enrichment in Svalbard, European High Arctic,  
947 Biogeochemistry, 98, 171-184, DOI 10.1007/s10533-009-9384-y, 2010.  
948 Hodson, A. J., Mumford, P. N., Kohler, J., and Wynn, P. M.: The High Arctic glacial ecosystem:  
949 new insights from nutrient budgets, Biogeochemistry, 72, 233-256, DOI 10.1007/s10533-  
950 004-0362-0, 2005.  
951 Ingwersen, J., Poll, C., Streck, T., and Kandeler, E.: Micro-scale modelling of carbon turnover  
952 driven by microbial succession at a biogeochemical interface, Soil Biol Biochem, 40, 864-878,  
953 DOI 10.1016/j.soilbio.2007.10.018, 2008.  
954 Insam, H., and Haselwandter, K.: Metabolic Quotient of the Soil Microflora in Relation to  
955 Plant Succession, Oecologia, 79, 174-178, Doi 10.1007/Bf00388474, 1989.  
956 Jakubas, D., Zmudzynska, K., Wojczulanis-Jakubas, K., and Stempniewicz, L.: Faeces  
957 deposition and numbers of vertebrate herbivores in the vicinity of planktivorous and  
958 piscivorous seabird colonies in Hornsund, Spitsbergen, Pol Polar Res, 29, 45-58, 2008.  
959 Jessup, C. M., Kassen, R., Forde, S. E., Kerr, B., Buckling, A., Rainey, P. B., and Bohannon, B. J.  
960 M.: Big questions, small worlds: microbial model systems in ecology, Trends Ecol Evol, 19,  
961 189-197, 10.1016/j.tree.2004.01.008, 2004.  
962 Johannessen, O. M., Bengtsson, L., Miles, M. W., Kuzmina, S. I., Semenov, V. A., Alekseev, G.  
963 V., Nagurnyi, A. P., Zakharov, V. F., Bobylev, L. P., Pettersson, L. H., Hasselmann, K., and  
964 Cattle, A. P.: Arctic climate change: observed and modelled temperature and sea-ice  
965 variability, Tellus A, 56, 328-341, DOI 10.1111/j.1600-0870.2004.00060.x, 2004.  
966 Kastovska, K., Elster, J., Stibal, M., and Santruckova, H.: Microbial assemblages in soil  
967 microbial succession after glacial retreat in Svalbard (high Arctic), Microbial Ecol, 50, 396-  
968 407, DOI 10.1007/s00248-005-0246-4, 2005.  
969 King, A. J., Meyer, A. F., and Schmidt, S. K.: High levels of microbial biomass and activity in  
970 unvegetated tropical and temperate alpine soils, Soil Biol Biochem, 40, 2605-2610, DOI  
971 10.1016/j.soilbio.2008.06.026, 2008.  
972 Kirchman, D.: Measuring Bacterial Biomass Production and Growth Rates from Leucine  
973 Incorporation in Natural Aquatic Environments in: Marine Microbiology, edited by: Paul, J.  
974 H., Academic Press, London, UK, 2001.  
975 Kirschke, S., Bousquet, P., Ciais, P., Saunois, M., Canadell, J. G., Dlugokencky, E. J.,  
976 Bergamaschi, P., Bergmann, D., Blake, D. R., Bruhwiler, L., Cameron-Smith, P., Castaldi, S.,  
977 Chevallier, F., Feng, L., Fraser, A., Heimann, M., Hodson, E. L., Houweling, S., Josse, B.,  
978 Fraser, P. J., Krummel, P. B., Lamarque, J. F., Langenfelds, R. L., Le Quere, C., Naik, V.,  
979 O'Doherty, S., Palmer, P. I., Pison, I., Plummer, D., Poulter, B., Prinn, R. G., Rigby, M.,  
980 Ringeval, B., Santini, M., Schmidt, M., Shindell, D. T., Simpson, I. J., Spahni, R., Steele, L. P.,  
981 Strode, S. A., Sudo, K., Szopa, S., van der Werf, G. R., Voulgarakis, A., van Weele, M., Weiss,  
982 R. F., Williams, J. E., and Zeng, G.: Three decades of global methane sources and sinks, Nat  
983 Geosci, 6, 813-823, Doi 10.1038/Ngeo1955, 2013.  
984 Knapp, E. B., Elliott, L. F., and Campbell, G. S.: Carbon, Nitrogen and Microbial Biomass  
985 Interrelationships during the Decomposition of Wheat Straw - a Mechanistic Simulation-  
986 Model, Soil Biol Biochem, 15, 455-461, Doi 10.1016/0038-0717(83)90011-1, 1983.  
987 Kuhnelt, R., Roberts, T. J., Bjorkman, M. P., Isaksson, E., Aas, W., Holmen, K., and Strom, J.:  
988 20-Year Climatology of NO<sub>3</sub>- and NH<sub>4</sub><sup>+</sup> Wet Deposition at Ny-Alesund, Svalbard, Adv  
989 Meteorol, Artn 406508  
990 Doi 10.1155/2011/406508, 2011.

991 Kuhnel, R., Bjorkman, M. P., Vega, C. P., Hodson, A., Isaksson, E., and Strom, J.: Reactive  
992 nitrogen and sulphate wet deposition at Zeppelin Station, Ny-Alesund, Svalbard, *Polar Res*,  
993 32, Unsp 19136  
994 Doi 10.3402/Polar.V32i0.19136, 2013.  
995 Larsen, P., Hamada, Y., and Gilbert, J.: Modeling microbial communities: Current,  
996 developing, and future technologies for predicting microbial community interaction, *J*  
997 *Biotechnol*, 160, 17-24, 10.1016/j.jbiotec.2012.03.009, 2012.  
998 Lazzaro, A., Brankatschk, R., and Zeyer, J.: Seasonal dynamics of nutrients and bacterial  
999 communities in unvegetated alpine glacier forefields, *Appl Soil Ecol*, 53, 10-22, DOI  
1000 10.1016/j.apsoil.2011.10.013, 2012.  
1001 Lazzaro, A., Hilfiker, D., and Zeyer, J.: Structures of Microbial Communities in Alpine Soils:  
1002 Seasonal and Elevational Effects, *Frontiers in microbiology*, 6, ARTN 1330  
1003 10.3389/fmicb.2015.01330, 2015.  
1004 Lee, S.: A theory for polar amplification from a general circulation perspective, *Asia-Pac J*  
1005 *Atmos Sci*, 50, 31-43, DOI 10.1007/s13143-014-0024-7, 2014.  
1006 Luoto, T. P., Oksman, M., and Ojala, A. E. K.: Climate change and bird impact as drivers of  
1007 High Arctic pond deterioration, *Polar Biol*, 38, 357-368, 10.1007/s00300-014-1592-9, 2015.  
1008 Lutz, S., Anesio, A. M., Villar, S. E. J., and Benning, L. G.: Variations of algal communities  
1009 cause darkening of a Greenland glacier, *Fems Microbiol Ecol*, 89, 402-414, 10.1111/1574-  
1010 6941.12351, 2014.  
1011 Lutz, S., Anesio, A. M., Edwards, A., and Benning, L. G.: Microbial diversity on Icelandic  
1012 glaciers and ice caps, *Frontiers in microbiology*, 6, ARTN 307  
1013 10.3389/fmicb.2015.00307, 2015.  
1014 Manzoni, S., Porporato, A., D'Odorico, P., Laio, F., and Rodriguez-Iturbe, I.: Soil nutrient  
1015 cycles as a nonlinear dynamical system, *Nonlinear Proc Geoph*, 11, 589-598, 2004.  
1016 Manzoni, S., and Porporato, A.: A theoretical analysis of nonlinearities and feedbacks in soil  
1017 carbon and nitrogen cycles, *Soil Biol Biochem*, 39, 1542-1556, 10.1016/j.soilbio.2007.01.006,  
1018 2007.  
1019 Mapelli, F., Marasco, R., Rizzi, A., Baldi, F., Ventura, S., Daffonchio, D., and Borin, S.: Bacterial  
1020 Communities Involved in Soil Formation and Plant Establishment Triggered by Pyrite  
1021 Bioweathering on Arctic Moraines, *Microbial Ecol*, 61, 438-447, 10.1007/s00248-010-9758-  
1022 7, 2011.  
1023 McDonald, D., Price, M. N., Goodrich, J., Nawrocki, E. P., DeSantis, T. Z., Probst, A.,  
1024 Andersen, G. L., Knight, R., and Hugenholtz, P.: An improved Greengenes taxonomy with  
1025 explicit ranks for ecological and evolutionary analyses of bacteria and archaea, *Isme J*, 6,  
1026 610-618, 10.1038/ismej.2011.139, 2012.  
1027 Michelutti, N., Keatley, B. E., Brimble, S., Blais, J. M., Liu, H. J., Douglas, M. S. V., Mallory, M.  
1028 L., Macdonald, R. W., and Smol, J. P.: Seabird-driven shifts in Arctic pond ecosystems, *P Roy*  
1029 *Soc B-Biol Sci*, 276, 591-596, 10.1098/rspb.2008.1103, 2009.  
1030 Michelutti, N., Mallory, M. L., Blais, J. M., Douglas, M. S. V., and Smol, J. P.: Chironomid  
1031 assemblages from seabird-affected High Arctic ponds, *Polar Biol*, 34, 799-812,  
1032 10.1007/s00300-010-0934-5, 2011.  
1033 Mindl, B., Anesio, A. M., Meirer, K., Hodson, A. J., Laybourn-Parry, J., Sommaruga, R., and  
1034 Sattler, B.: Factors influencing bacterial dynamics along a transect from supraglacial runoff  
1035 to proglacial lakes of a high Arctic glacier (vol 7, pg 307, 2007), *Fems Microbiol Ecol*, 59,  
1036 762-762, DOI 10.1111/j.1574-6941.2007.00295.x, 2007.

1037 Moe, B., Stempniewicz, L., Jakubas, D., Angelier, F., Chastel, O., Dinessen, F., Gabrielsen, G.  
1038 W., Hanssen, F., Karnovsky, N. J., Ronning, B., Welcker, J., Wojczulanis-Jakubas, K., and Bech,  
1039 C.: Climate change and phenological responses of two seabird species breeding in the high-  
1040 Arctic, *Mar Ecol Prog Ser*, 393, 235-246, 10.3354/meps08222, 2009.

1041 Moreau, M., Mercier, D., Laffly, D., and Roussel, E.: Impacts of recent paraglacial dynamics  
1042 on plant colonization: A case study on Midtre Lovénbreen foreland, Spitsbergen (79 degrees  
1043 N), *Geomorphology*, 95, 48-60, DOI 10.1016/j.geomorph.2006.07.031, 2008.

1044 Moritz, R. E., Bitz, C. M., and Steig, E. J.: Dynamics of recent climate change in the Arctic,  
1045 *Science*, 297, 1497-1502, DOI 10.1126/science.1076522, 2002.

1046 Oechel, W. C., Hastings, S. J., Vourlitis, G., Jenkins, M., Riechers, G., and Grulke, N.: Recent  
1047 Change of Arctic Tundra Ecosystems from a Net Carbon-Dioxide Sink to a Source, *Nature*,  
1048 361, 520-523, DOI 10.1038/361520a0, 1993.

1049 Oechel, W. C., Vourlitis, G. L., Hastings, S. J., Zulueta, R. C., Hinzman, L., and Kane, D.:  
1050 Acclimation of ecosystem CO<sub>2</sub> exchange in the Alaskan Arctic in response to decadal climate  
1051 warming, *Nature*, 406, 978-981, Doi 10.1038/35023137, 2000.

1052 Paul, F., Frey, H., and Le Bris, R.: A new glacier inventory for the European Alps from Landsat  
1053 TM scenes of 2003: challenges and results, *Ann Glaciol*, 52, 144-152, 2011.

1054 Prietzel, J., Dumig, A., Wu, Y. H., Zhou, J., and Klysubun, W.: Synchrotron-based P K-edge  
1055 XANES spectroscopy reveals rapid changes of phosphorus speciation in the topsoil of two  
1056 glacier foreland chronosequences, *Geochim Cosmochim Acta*, 108, 154-171, DOI  
1057 10.1016/j.gca.2013.01.029, 2013.

1058 Schipper, L. A., Hobbs, J. K., Rutledge, S., and Arcus, V. L.: Thermodynamic theory explains  
1059 the temperature optima of soil microbial processes and high Q(10) values at low  
1060 temperatures, *Global Change Biol*, 20, 3578-3586, Doi 10.1111/Gcb.12596, 2014.

1061 Schloss, P. D., Westcott, S. L., Ryabin, T., Hall, J. R., Hartmann, M., Hollister, E. B., Lesniewski,  
1062 R. A., Oakley, B. B., Parks, D. H., Robinson, C. J., Sahl, J. W., Stres, B., Thallinger, G. G., Van  
1063 Horn, D. J., and Weber, C. F.: Introducing mothur: Open-Source, Platform-Independent,  
1064 Community-Supported Software for Describing and Comparing Microbial Communities, *Appl  
1065 Environ Microb*, 75, 7537-7541, 10.1128/Aem.01541-09, 2009.

1066 Schmidt, S. K., Reed, S. C., Nemergut, D. R., Grandy, A. S., Cleveland, C. C., Weintraub, M. N.,  
1067 Hill, A. W., Costello, E. K., Meyer, A. F., Neff, J. C., and Martin, A. M.: The earliest stages of  
1068 ecosystem succession in high-elevation (5000 metres above sea level), recently deglaciated  
1069 soils, *P Roy Soc B-Biol Sci*, 275, 2793-2802, DOI 10.1098/rspb.2008.0808, 2008.

1070 Schostag, M., Stibal, M., Jacobsen, C. S., Baelum, J., Tas, N., Elberling, B., Jansson, J. K.,  
1071 Semenchuk, P., and Prieme, A.: Distinct summer and winter bacterial communities in the  
1072 active layer of Svalbard permafrost revealed by DNA- and RNA-based analyses, *Frontiers in  
1073 microbiology*, 6, ARTN 399  
1074 10.3389/fmicb.2015.00399, 2015.

1075 Schulz, S., Brankatschk, R., Dumig, A., Kogel-Knabner, I., Schloter, M., and Zeyer, J.: The role  
1076 of microorganisms at different stages of ecosystem development for soil formation,  
1077 *Biogeosciences*, 10, 3983-3996, DOI 10.5194/bg-10-3983-2013, 2013.

1078 Schutte, U. M. E., Abdo, Z., Bent, S. J., Williams, C. J., Schneider, G. M., Solheim, B., and  
1079 Forney, L. J.: Bacterial succession in a glacier foreland of the High Arctic, *Isme J*, 3, 1258-  
1080 1268, DOI 10.1038/ismej.2009.71, 2009.

1081 Scott, E. M., Rattray, E. A. S., Prosser, J. I., Killham, K., Glover, L. A., Lynch, J. M., and Bazin,  
1082 M. J.: A Mathematical-Model for Dispersal of Bacterial Inoculants Colonizing the Wheat  
1083 Rhizosphere, *Soil Biol Biochem*, 27, 1307-1318, Doi 10.1016/0038-0717(95)00050-O, 1995.

1084 Serreze, M. C., Walsh, J. E., Chapin, F. S., Osterkamp, T., Dyurgerov, M., Romanovsky, V.,  
1085 Oechel, W. C., Morison, J., Zhang, T., and Barry, R. G.: Observational evidence of recent  
1086 change in the northern high-latitude environment, *Climatic Change*, 46, 159-207, Doi  
1087 10.1023/A:1005504031923, 2000.

1088 Servedio, M. R., Brandvain, Y., Dhole, S., Fitzpatrick, C. L., Goldberg, E. E., Stern, C. A., Van  
1089 Cleve, J., and Yeh, D. J.: Not just a theory--the utility of mathematical models in evolutionary  
1090 biology, *Plos Biol*, 12, e1002017, 10.1371/journal.pbio.1002017, 2014.

1091 Simon, M., and Azam, F.: Protein-Content and Protein-Synthesis Rates of Planktonic Marine-  
1092 Bacteria, *Mar Ecol Prog Ser*, 51, 201-213, DOI 10.3354/meps051201, 1989.

1093 Smittenberg, R. H., Gierga, M., Goransson, H., Christl, I., Farinotti, D., and Bernasconi, S. M.:  
1094 Climate-sensitive ecosystem carbon dynamics along the soil chronosequence of the Damma  
1095 glacier forefield, Switzerland, *Global Change Biol*, 18, 1941-1955, DOI 10.1111/j.1365-  
1096 2486.2012.02654.x, 2012.

1097 Soetaert, K., and Herman, P.: *A Practical Guide to Ecological Modelling: Using R as a*  
1098 *Simulation Platform*, Springer, UK, 2009.

1099 Staines, K. E. H., Carrivick, J. L., Tweed, F. S., Evans, A. J., Russell, A. J., Jóhannesson, T., and  
1100 Roberts, M.: A multi-dimensional analysis of pro-glacial landscape change at Sólheimajökull,  
1101 southern Iceland, *Earth Surface Processes and Landforms*, 40, 809-822, 10.1002/esp.3662,  
1102 2014.

1103 Stapleton, L. M., Crout, N. M. J., Sawstrom, C., Marshall, W. A., Poulton, P. R., Tye, A. M.,  
1104 and Laybourn-Parry, J.: Microbial carbon dynamics in nitrogen amended Arctic tundra soil:  
1105 Measurement and model testing, *Soil Biol Biochem*, 37, 2088-2098, DOI  
1106 10.1016/j.soilbio.2005.03.016, 2005.

1107 Stibal, M., Tranter, M., Benning, L. G., and Rehak, J.: Microbial primary production on an  
1108 Arctic glacier is insignificant in comparison with allochthonous organic carbon input, *Environ*  
1109 *Microbiol*, 10, 2172-2178, 10.1111/j.1462-2920.2008.01620.x, 2008.

1110 Strauss, S. L., Garcia-Pichel, F., and Day, T. A.: Soil microbial carbon and nitrogen  
1111 transformations at a glacial foreland on Anvers Island, Antarctic Peninsula, *Polar Biol*, 35,  
1112 1459-1471, DOI 10.1007/s00300-012-1184-5, 2012.

1113 Telling, J., Anesio, A. M., Tranter, M., Irvine-Fynn, T., Hodson, A., Butler, C., and Wadham, J.:  
1114 Nitrogen fixation on Arctic glaciers, Svalbard, *J Geophys Res-Biogeophys*, 116, Artn G03039  
1115 Doi 10.1029/2010jg001632, 2011.

1116 Telling, J., Stibal, M., Anesio, A. M., Tranter, M., Nias, I., Cook, J., Bellas, C., Lis, G., Wadham,  
1117 J. L., Sole, A., Nienow, P., and Hodson, A.: Microbial nitrogen cycling on the Greenland Ice  
1118 Sheet, *Biogeosciences*, 9, 2431-2442, 10.5194/bg-9-2431-2012, 2012.

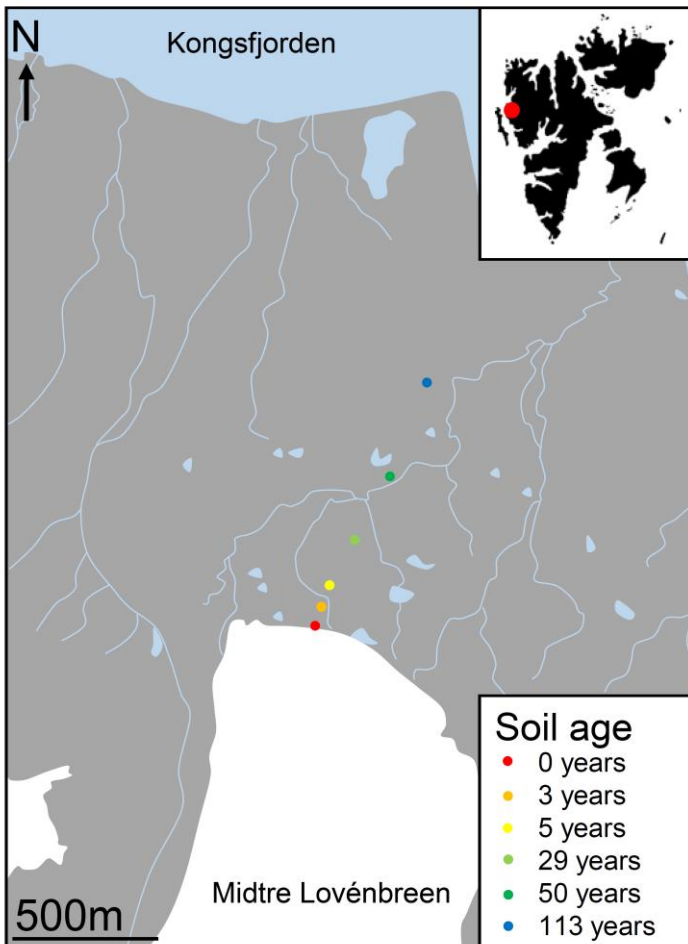
1119 Toal, M. E., Yeomans, C., Killham, K., and Meharg, A. A.: A review of rhizosphere carbon flow  
1120 modelling, *Plant Soil*, 222, 263-281, Doi 10.1023/A:1004736021965, 2000.

1121 Tscherko, D., Rustemeier, J., Richter, A., Wanek, W., and Kandeler, E.: Functional diversity of  
1122 the soil microflora in primary succession across two glacier forelands in the Central Alps, *Eur*  
1123 *J Soil Sci*, 54, 685-696, DOI 10.1046/j.1365-2389.2003.00570.x, 2003.

1124 Vandewerf, H., and Verstraete, W.: Estimation of Active Soil Microbial Biomass by  
1125 Mathematical-Analysis of Respiration Curves - Development and Verification of the Model,  
1126 *Soil Biol Biochem*, 19, 253-260, Doi 10.1016/0038-0717(87)90006-X, 1987.

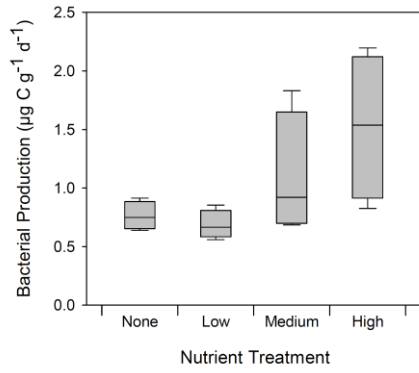
1127 Wang, Y. P., Chen, B. C., Wieder, W. R., Leite, M., Medlyn, B. E., Rasmussen, M., Smith, M. J.,  
1128 Augusto, F. B., Hoffman, F., and Luo, Y. Q.: Oscillatory behavior of two nonlinear microbial  
1129 models of soil carbon decomposition, *Biogeosciences*, 11, 1817-1831, 10.5194/bg-11-1817-  
1130 2014, 2014.

1131 Yde, J. C., Finster, K. W., Raiswell, R., Steffensen, J. P., Heinemeier, J., Olsen, J.,  
1132 Gunnlaugsson, H. P., and Nielsen, O. B.: Basal ice microbiology at the margin of the  
1133 Greenland ice sheet, *Ann Glaciol*, 51, 71-79, 2010.  
1134 Yoshitake, S., Uchida, M., Koizumi, H., Kanda, H., and Nakatsubo, T.: Production of biological  
1135 soil crusts in the early stage of primary succession on a High Arctic glacier foreland, *New*  
1136 *Phytol*, 186, 451-460, DOI 10.1111/j.1469-8137.2010.03180.x, 2010.  
1137 Zdanowski, M. K., Zmuda-Baranowska, M. J., Borsuk, P., Swiatecki, A., Gorniak, D., Wolicka,  
1138 D., Jankowska, K. M., and Grzesiak, J.: Culturable bacteria community development in  
1139 postglacial soils of Ecology Glacier, King George Island, Antarctica, *Polar Biol*, 36, 511-527,  
1140 DOI 10.1007/s00300-012-1278-0, 2013.  
1141 Zelenev, V. V., van Bruggen, A. H. C., and Semenov, A. M.: "BACWAVE," a spatial-temporal  
1142 model for traveling waves of bacterial populations in response to a moving carbon source in  
1143 soil, *Microbial Ecol*, 40, 260-272, 2000.  
1144 Zhang, X. Y., Wang, W., Chen, W. L., Zhang, N. L., and Zeng, H.: Comparison of Seasonal Soil  
1145 Microbial Process in Snow-Covered Temperate Ecosystems of Northern China, *Plos One*, 9,  
1146 ARTN e92985  
1147 10.1371/journal.pone.0092985, 2014.  
1148 Ziolek, M., and Melke, J.: The impact of seabirds on the content of various forms of  
1149 phosphorus in organic soils of the Bellsund coast, western Spitsbergen, *Polar Res*, 33, ARTN  
1150 19986  
1151 10.3402/polar.v33.19986, 2014.  
1152 Zumsteg, A., Bernasconi, S. M., Zeyer, J., and Frey, B.: Microbial community and activity  
1153 shifts after soil transplantation in a glacier forefield, *Appl Geochem*, 26, S326-S329, DOI  
1154 10.1016/j.apgeochem.2011.03.078, 2011.  
1155 Zumsteg, A., Luster, J., Goransson, H., Smittenberg, R. H., Brunner, I., Bernasconi, S. M.,  
1156 Zeyer, J., and Frey, B.: Bacterial, Archaeal and Fungal Succession in the Forefield of a  
1157 Receding Glacier, *Microbial Ecol*, 63, 552-564, DOI 10.1007/s00248-011-9991-8, 2012.  
1158 Zumsteg, A., Schmutz, S., and Frey, B.: Identification of biomass utilizing bacteria in a  
1159 carbon-depleted glacier forefield soil by the use of <sup>13</sup>C DNA stable isotope probing, *Env*  
1160 *Microbiol Rep*, 5, 424-437, Doi 10.1111/1758-2229.12027, 2013.  
1161  
1162  
1163  
1164  
1165  
1166  
1167  
1168

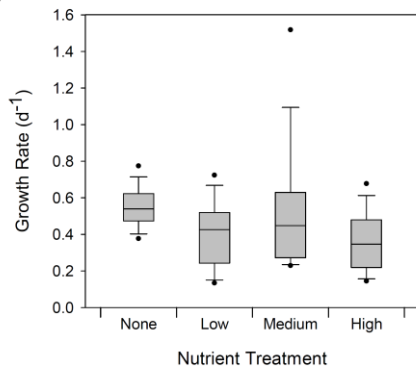


1169  
 1170 Figure 1. Midtre Lovénbreen glacier and forefield in Svalbard, the location of sampling sites and  
 1171 approximate age of soil.  
 1172

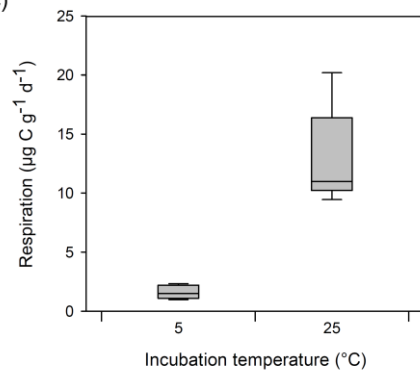
(a)



(b)



(c)



1173

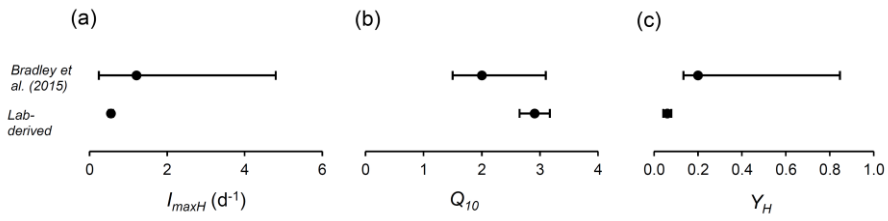
1174 Figure 2. Measurements of (a) bacterial carbon production and (b) growth rate, derived from  $^3\text{H}$ -

1175 leucine assays at different nutrient conditions, and (c) bacterial respiration at 5°C and 25°C.

1176

1177

1178



1179

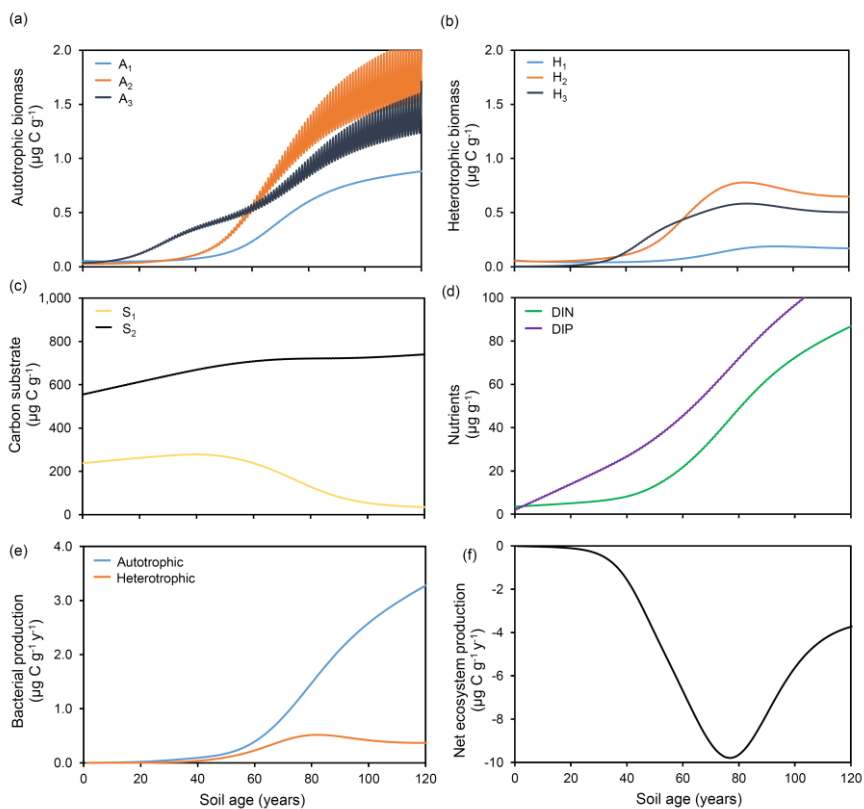
1180

1181

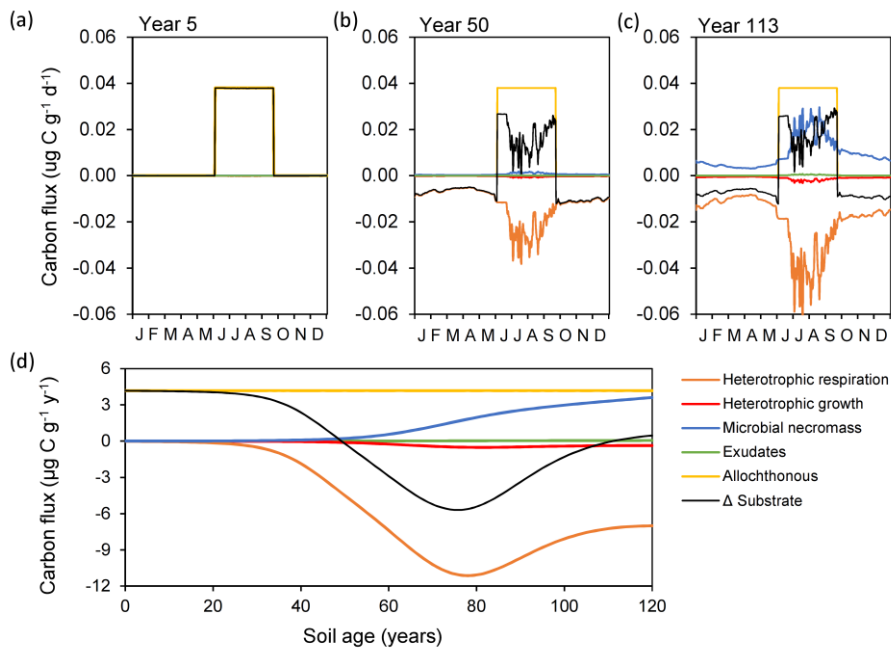
1182 Figure 3. A comparison of previously established ranges for parameters (Bradley et al., 2015) with  
1183 laboratory-derived values for (a) maximum growth rate ( $I_{max}$ ), (b) temperature response ( $Q_{10}$ ), (c) BGE  
1184 ( $Y$ ).

1185

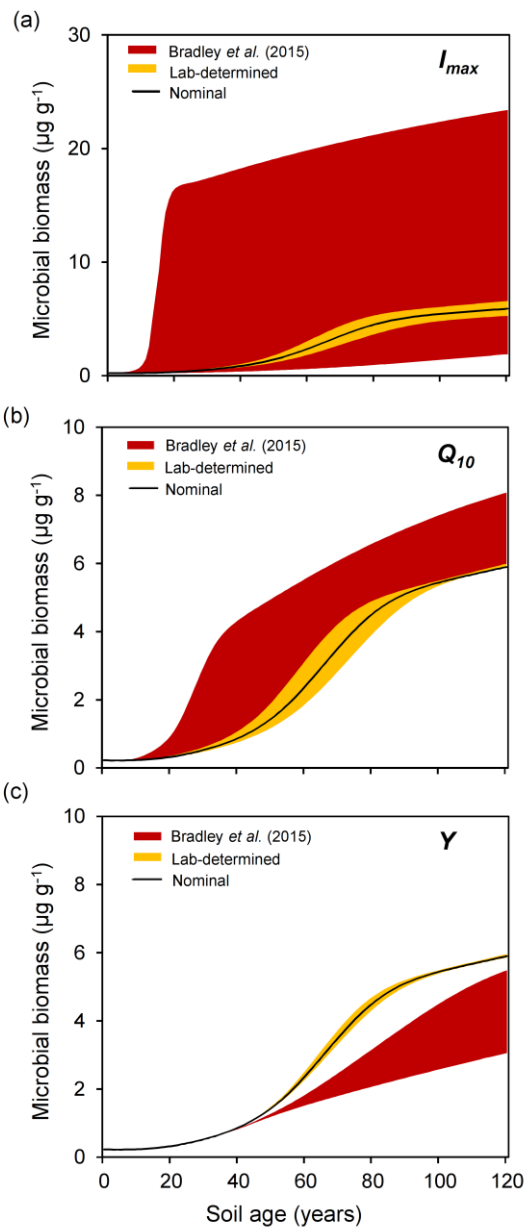




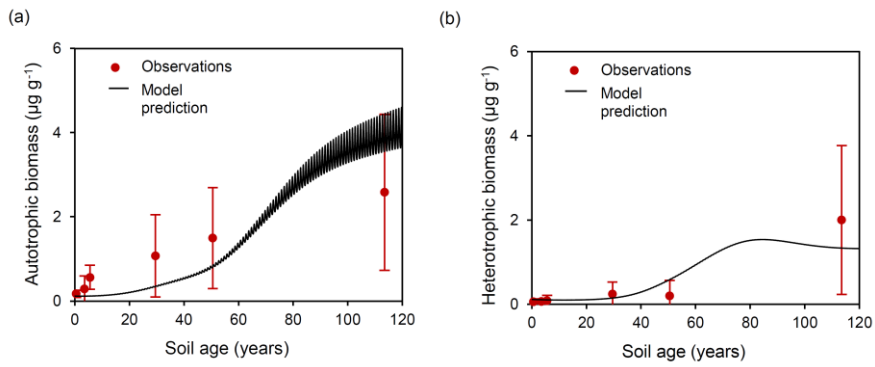
1186  
 1187 Figure 4. Modelled (a) autotrophic biomass, (b) heterotrophic biomass, (c) carbon substrate, (d)  
 1188 nutrients, (e) bacterial production and (f) CO<sub>2</sub> effluxnet ecosystem production, with laboratory-derived  
 1189 parameter values.  
 1190



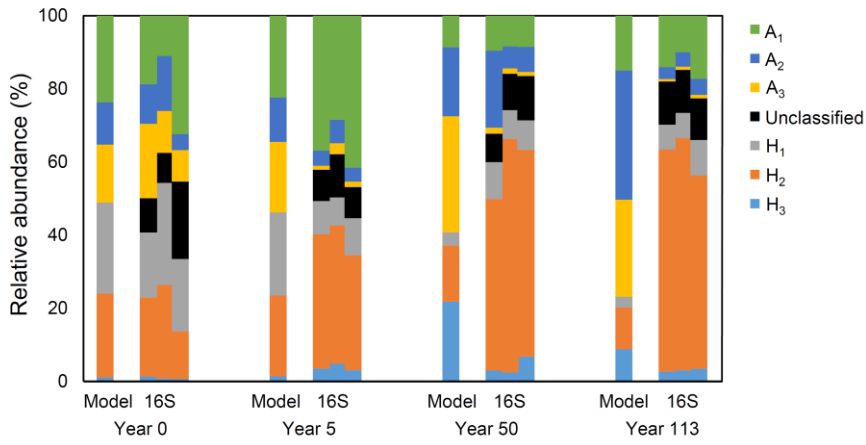
1191  
 1192 Figure 5. Illustration of daily carbon fluxes for (a) 5, (b) 50 and (c) 113 year old soil, and (d) annual  
 1193 carbon flux over 120 years. Microbial necromass (blue), exudates (green) and allochthonous sources  
 1194 (yellow) contribute to the substrate pool (black), and heterotrophic growth (red) and respiration  
 1195 (orange) deplete it.  
 1196



1197  
 1198 Figure 6. A comparison of predicted microbial biomass with laboratory-derived parameter values  
 1199 (yellow) and previously established parameter values (Bradley et al., 2015) (red) for variation in the  
 1200 following parameters: (a) maximum growth rate ( $I_{max}$ ), (b) temperature response ( $Q_{10}$ ), (c) BGE ( $Y$ ).  
 1201



1202  
 1203 Figure 7. Model predictions of (a) autotrophic and (b) heterotrophic biomass (black line), compared to  
 1204 observational data (red) derived from microscopy.  
 1205



1206  
 1207 Figure 8. A comparison of microbial diversity from model output and genomic analyses at 0 year old,  
 1208 5 year old, 50 year old and 113 year old soil.  
 1209  
 1210  
 1211

1212

1213 Table 1. State variables and initial values.

State Variable	Units	Description	Initial value (year 0) ( $\mu\text{g g}^{-1}$ )
$A_1$	$\mu\text{g C g}^{-1}$	Subglacial chemolithoautotrophs	0.0547
$A_2$	$\mu\text{g C g}^{-1}$	Soil autotrophs	0.0266
$A_3$	$\mu\text{g C g}^{-1}$	Nitrogen fixing soil autotrophs	0.0355
$H_1$	$\mu\text{g C g}^{-1}$	Subglacial heterotrophs	0.0576
$H_2$	$\mu\text{g C g}^{-1}$	Soil heterotrophs	0.0530
$H_3$	$\mu\text{g C g}^{-1}$	Nitrogen fixing soil heterotrophs	0.0025
$S_1$	$\mu\text{g C g}^{-1}$	Labile organic carbon	291.895
$S_2$	$\mu\text{g C g}^{-1}$	Refractory organic carbon	681.089
DIN	$\mu\text{g N g}^{-1}$	Dissolved inorganic nitrogen (DIN)	3.530
DIP	$\mu\text{g P g}^{-1}$	Dissolved inorganic phosphorus (DIP)	2.078
$ON_1$	$\mu\text{g N g}^{-1}$	Labile organic nitrogen	41.157
$ON_2$	$\mu\text{g N g}^{-1}$	Refractory organic nitrogen	96.034
$OP_1$	$\mu\text{g P g}^{-1}$	Labile organic phosphorus	24.227
$OP_2$	$\mu\text{g P g}^{-1}$	Refractory organic phosphorus	56.530

1214

1215

1216

1217

1218 Table 2. Microbial biomass in the forefield of Midtre Lovénbreen (brackets show 1 standard deviation)  
 1219

Soil Age (years)	Autotrophic biomass ( $\mu\text{g C g}^{-1}$ )	Heterotrophic biomass ( $\mu\text{g C g}^{-1}$ )	Total Organic Carbon ( $\mu\text{g C g}^{-1}$ )
0	0.171 (0.042)	0.059 (0.034)	792.984 (127.206)
3	0.287 (0.155)	0.064 (0.029)	
5	0.561 (0.143)	0.083 (0.065)	
29	1.072 (0.487)	0.244 (0.142)	
50	1.497 (0.601)	0.197 (0.184)	
113	2.581 (0.927)	2.000 (0.885)	

1220  
 1221  
 1222  
 1223  
 1224  
 1225

1226

Table 3. Model output.

Soil Age (years)	Autotrophic biomass ( $\mu\text{g C g}^{-1}$ )	Heterotrophic biomass ( $\mu\text{g C g}^{-1}$ )	Autotrophic production ( $\mu\text{g C g}^{-1} \text{y}^{-1}$ )	Heterotrophic production ( $\mu\text{g C g}^{-1} \text{y}^{-1}$ )	Net $\text{CO}_2$ efflux from ecosystem production ( $\mu\text{g C g}^{-1} \text{y}^{-1}$ )	DIN assimilation ( $\mu\text{g N g}^{-1} \text{y}^{-1}$ )	$\text{N}_2$ fixation ( $\mu\text{g N g}^{-1} \text{y}^{-1}$ )
0	0.117	0.111	0.002	0.001	-0.011	$2.0 \times 10^{-4}$	$2.0 \times 10^{-4}$
3	0.117	0.105	0.003	0.001	-0.020	$3.0 \times 10^{-4}$	$3.0 \times 10^{-4}$
5	0.119	0.102	0.004	0.001	-0.025	$4.0 \times 10^{-4}$	$4.0 \times 10^{-4}$
29	0.359	0.147	0.050	0.012	-0.391	0.002	0.006
50	0.860	0.591	0.187	0.113	-4.311	0.022	0.021
113	4.414	1.331	3.093	0.376	-4.031	0.458	0.031

1227

1228

1229

1230

1231

1232

1233